IAEA
International Atomic Energy Agency

INDC(EGY)-008
Distr. G

INDC International Nuclear Data Committee

RESEARCH STUDIES PERFORMED USING THE CAIRO FOURIER DIFFRACTOMETER FACILITY

R. M. A. Maayouf
Reactor Physics Department, NRC
Atomic Energy Authority
Cairo, Egypt

Edited by D. Ridikas, IAEA - Physics Section, Vienna, Austria

December 2009

IAEA Nuclear Data Section, Vienna International Centre, A-1400 Vienna, Austria

Selected INDC documents may be downloaded in electronic form from
http://www-nds.iaea.org/indc_sel.html or sent as an e-mail attachment.
Requests for hardcopy or e-mail transmittal should be directed to *services@iaeand.iaea.org*
or to:
Nuclear Data Section
International Atomic Energy Agency
Vienna International Centre
PO Box 100
A-1400 Vienna
Austria

Printed by the IAEA in Austria

December 2009

INDC(EGY)-008
Distr. G

RESEARCH STUDIES PERFORMED USING THE CAIRO FOURIER DIFFRACTOMETER FACILITY

R. M. A. Maayouf
Reactor Physics Department, NRC
Atomic Energy Authority
Cairo, Egypt

Edited by D. Ridikas, IAEA - Physics Section, Vienna, Austria

ABSTRACT

This report represents the results of the research studies performed using the Cairo Fourier Diffractometer Facility (CFDF), within 10 years after it was installed and put into operation at the beginning of 1996. The main components of the CFDF were supplied by the IAEA according to the technical assistance project EGY/1/022 "Upgrading of Research Reactor Utilization". The present report is the second published INDC report, while the first one, published at the beginning of 1997, was about the performance of the CFDF and its main characteristic parameters. Plenty of measurements were performed since then, yielding several publications both in local and international scientific periodicals and resulting in 8 M.Sc. and Ph.D. degrees from Egyptian Universities. In addition, a new approach for the analysis of the neutron spectra was implemented using the CFDF. Specially designed interface card with proper software program was applied instead of the reverse time of flight (RTOF) and Finnish made analyzer originally attached to the facility. It has been verified that the new approach can successfully replace the RTOF analyzer, significantly decreasing the time of measurement and saving the reactor's operation time. Besides, a special fault diagnostic system program was developed and tested for caring and handling the possible failures of the CFDF. Moreover, measurements were carried out for the diffraction spectra emitted at different points of one of the samples. The latter was scanned across the neutron beam of the CFDF, for studying the stress after welding; used in industrial applications.

December 2009

CONTENTS

INTRODUCTION **7**

1. THE CFDF ARRANGEMENT **8**

2. MEASUREMENTS USING THE CFDF **9**

2.1. Measurements with the NG Facility 9

2.2. Optimization of the detection system 11

2.3. On the resolution of the CFDF 16

2.4. Measurements for Stress Analysis 18

3. NEW DEVELOPMENTS OF THE CFDF **20**

4. FAULT DIAGNOSTIC SYSTEM **27**

5. THE DEVELOPMENT OF PLASTIC NEUTRON MIRRORS **31**

5.1. Experimental details 31

5.2. Results and discussion 32

6. CONCLUSIONS **37**

7. ACKNOWLEDGEMENTS **38**

8. REFERENCES **39**

9. LIST OF DISSERTATIONS PERFORMED USING THE CFDF (SUPERVISED BY PROF. DR. R.M.A. MAAYOUF) **41**

Introduction

The properties of condensed matter can be efficiently studied through the scattering of slow neutrons, since both their energy and wavelength match the atomic energies and distances characteristic for condensed matter. The time of flight (TOF) method has been successfully used for such purpose, as it allows studying the sample at exceptional conditions, for example at high pressure or temperature. Correlation TOF methods using either Fourier or pseudo-random beam modulation, have been developed to use the available neutron flux in a way more economic than with the usual Fermi chopper systems; and without deterioration of the resolution.

The Fourier approach allows for a duty factor up to 50 % while the Fermi chopper systems make use only of ~0.1-0.5% of the available neutrons [1; 2]. The Fourier method has been improved by the reverse time-of-flight (RTOF) concept [3-5] which is based on the triggering of the TOF analyzer by the detected neutrons instead of the rotor's position.

The use of the Fourier RTOF diffractometry as efficient tool for studying condensed matter at the ET-RR-1 reactor was first assessed by Maayouf [1], and the preliminary arrangements to be used at such type of reactor were also given by him. Further developments of the suggested arrangement were also represented in various articles by Maayouf [6-10], along with the main components required for the data acquisition. Moreover, the basic stage of the Cairo Fourier Diffractometer Facility (CFDF), based on the RTOF concept, was installed at the beginning of 1996, as IAEA-TC Project EGY/1/022, at one of the horizontal channels of the ET-RR-1 reactor. The CFDF is one of the four [11-14] functioning Fourier diffractometers.

1. The CFDF arrangement

A schematic diagram of the CFDF at the ET-RR-1 reactor is represented in Figure 1. Neutrons emitted through an in-pile collimator, from one of the ET-RR-1 reactor horizontal channels, are at first guided by the main neutron guide (22 m in length), and then reach the Fourier chopper. After the Fourier chopper, neutrons pass through an auxiliary neutron guide (3 m long) to the sample. Neutrons scattered from the sample at 90° are detected by the detection system. The detector position in the mode of operation at this stage is at 90° scattering angle. The latter gives the best resolution in space localization of a sample scattering volume and could be efficiently used for studying the internal stresses in materials including neutron diffraction.

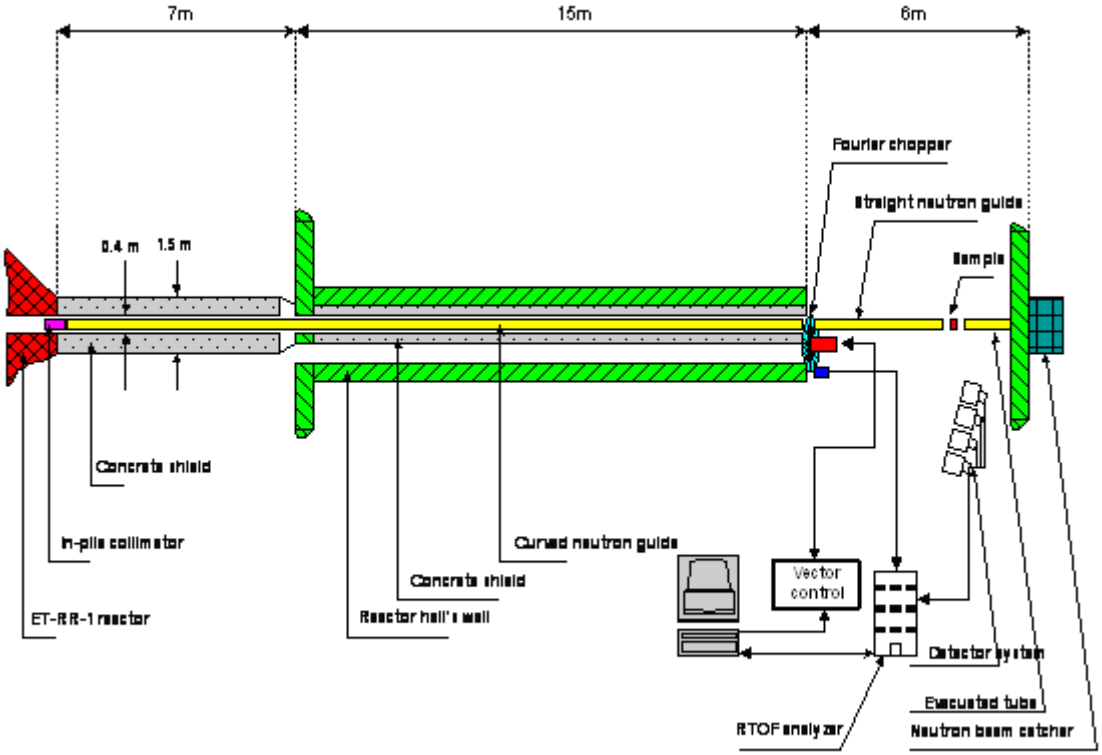

Fig. 1. Schematic diagram of the CFDF at the ET-RR-1 reactor.

The arrangement is also equipped with a Fermi chopper which could be used for spectrum measurements, etc. The Fermi chopper has been described in the IAEA report [15]. Preliminary reports on the performance and main characteristic parameters of the CFDF, measured just after the start of operation, were also made by Maayouf [15 -17]. The main parameters of the CFDF are given in Table 1.

2. Measurements using the CFDF

Different measurements were performed using the CFDF after its operation at the beginning of 1996. Part of the measurements targeted on the careful study of its important components such as the neutron guide (NG) facility, sample dimensions, detection system, and determination of the neutron flux using different detectors.

Table 1 The CFDF parameters.

Parameter	Value
λ range (Å)	1-4
D range (Å)	0.5-3.0
Φ_s (n / cm^2 s)	$1.1x10^6$
$V_s(cm^3)$	2.125
Resolution (%)	0.45
Ω (Steradian)	0.051
$\Phi_s V_s \Omega$ ($n.cm.s^{-1}$)	$1.2x10^5$

2.1. Measurements with the NG Facility

The NG Facility, as attached to the CFDF, has been described earlier [15] in details. It consists of a curved NG (22 m long, 3385.5 m radius of curvature) for delivering neutrons free from gamma rays and fast neutrons background to the Fourier chopper, and a straight NG (3 m long) for collimation of the beam incident on the sample under investigation. Both curved and straight NG have the same cross-sectional area (0.0135x0.09 m^2) of the mirror channel walls, which are coated with ^{58}Ni (2200 Å thick) as a reflecting surface.

The integral neutron flux and spectrum measurements were carried out for the evaluation of the performance of the NG facility [18; 19]. The neutron flux measurements were performed at the exit of the curved NG, and after the straight one, using both activated gold foils and calibrated detector methods. The calibrated detector measurements also were reported [15]. The activated gold foil measurements were carried out by the irradiation of gold foils (~16 mg weight) by neutron beam. The resulting activity due to irradiation by neutrons was measured using a gamma-ray spectrometer constructed of coaxial high purity Germanium (HPGe) described in details by Hashem [20]. Thus, using the known formula for activated gold foils method the integral neutron flux was determined, both at the exits of the curved NG and straight one [21]. The comparison of the determined values of the neutron flux and those ones previously measured using calibrated detector is given in Table 2.

The neutron beam spectrum measurement was carried out using Fermi disk type chopper. The Fermi chopper was rotating at 2840 rpm speed and the used detector was a ^{6}Li-glass scintillator (NE-912) set at 3.46 m distance from the chopper. The measured spectrum was reported in [15], along with the details of the measurement. The measured spectrum was corrected, taking into consideration the transmission of the chopper, counting losses due to detection system, and losses due to absorption and scattering out of 3.46 m column of the air molecules.

Table 2: The values of the neutron flux.

Point of measurement	Flux values using gold foil activation	Flux values using calibrated detector
At the exit of curved NGT	(6.71 ± 0.06) 10^6 n/ cm².s	(6.66 ± 0.32) 10^6 n/cm².s
At the exit of the straight NGT	(1.13 ± 0.02) 10^6 n/ cm².s	
At the sample position with rotating Fourier chopper		(1.05±0.05) 10^6 n/cm².s
At the sample position with open Fourier chopper		(2.1 ± 0.01) 10^6 n/cm².s

The values of the integral neutron flux, measured both by calibrated detector and activated gold foils method, are consistent (see Table 2). The neutron losses, within 28 cm distance between the exit of the straight NG and the sample position, are ~ 6.3%. As the result of the scattering and absorption out of the beam by air molecules, corresponding losses are estimated to be ~ 1.4 %, while the losses due to the beam divergence are ~ 4.9 %. The value of the neutron flux ($1.05x10^{-6}$ n/cm².s) at the sample position is slightly less than the value $1.2x10^{-6}$ n/cm².s reported [2; 13] for the FSS facility which is installed at the 5 MW reactor of the GKSS Centre (Germany). Besides, the neutron losses due to the beam divergence in case of the FSS facility are ~36.4%. This is in favor of the CFDF which is attached to a 2 MW reactor. Moreover, the reflecting surface of the FSS neutron guide is made from the natural Ni.

The effect of using natural Ni as reflecting surface, instead of ^{58}Ni, was studied through the ratio F (λ) between the neutron intensity transmitted by the NG in case of natural Ni coating and that one in case of ^{58}Ni. The calculated ratio is represented in Figure 2a. Consequently, the neutron intensity will be reduced according to the wavelength dependent factor F (λ) using natural Ni instead of ^{58}Ni. Besides, in case of Ni^{58} the neutron spectrum was calculated, from the present corrected spectrum considering the integral neutron flux value ~6.7x10-6 n/cm².s measured at the exit of the curved NG; following the procedure given in Trunov's report [22]. Both spectra are displayed in Figure 2b. The comparison between both spectra, (Figure 2b) is in favor of ^{58}Ni as the neutron intensity is ~1.4 times higher than that with the natural Ni. This shows the advantage of the NG facility attached to the CFDF. More details about the characteristics of the reflecting surface of the NG walls can be found in other sources [23].

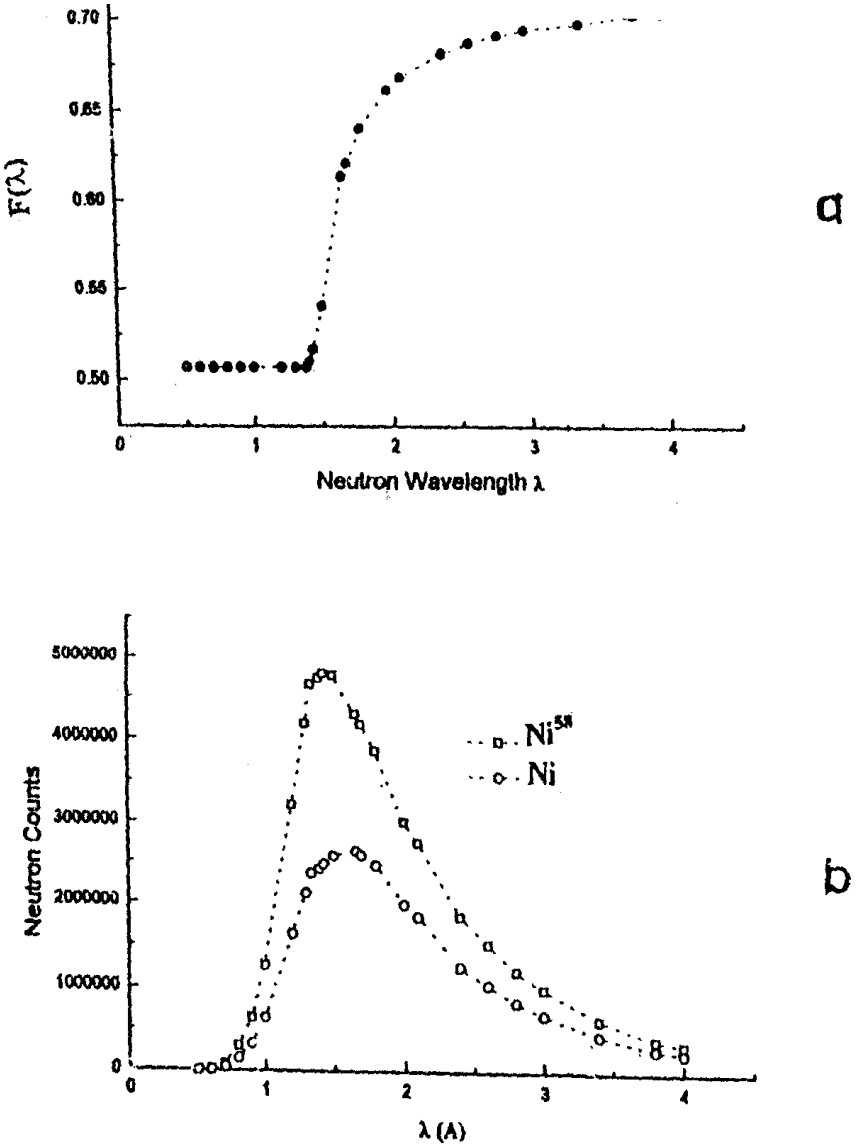

Fig. 2. a) The wavelength dependent factor F (λ);
b) Neutron spectra from the curved NG facility in case of ^{58}Ni and Ni.

2.2. Optimization of the detection system

The detection system of the CFDF is designed for detecting neutrons scattered from the sample at an angle 2θ=90° and consists of four independent scintillation detector elements (see Fig. 3). The detection system aperture is determined by the area of all four elements, their angular positions and their distance from the sample. Consequently, the detector elements have to be arranged according to the time focusing geometry, in order to increase the luminosity of the diffractometer for the given resolution. Each of the detector elements is made of 1mm thick ^{6}Li-glass scintillator (NE-912) whose surface area is 200*200 mm². The actual values of the CFDF detector elements parameters are represented in Figure 3.

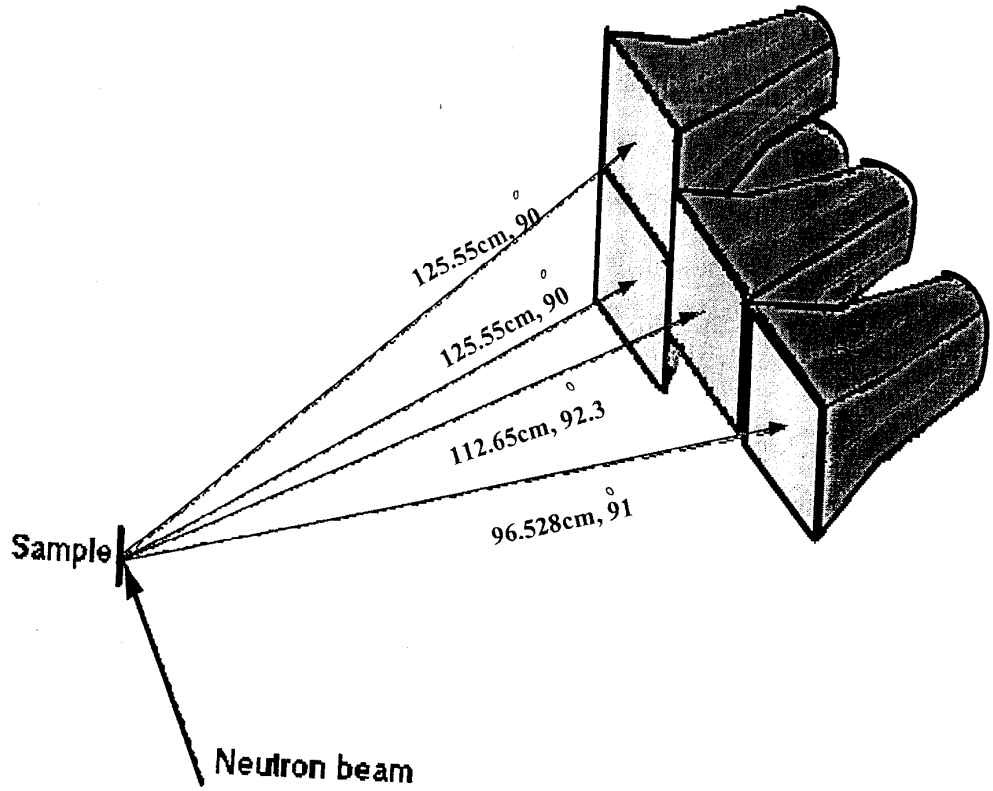

Fig. 3: A schematic of the four elements of the detection system.

The locus of constant time of arrival for the detection system is represented in Figure 4. The time focusing surface is uniquely defined by the constants A_0, B_0 and θ_0, where the locus of constant time arrival and the angle between the tangent to the locus and the incident beam direction are given by the formula derived in ref [24]. Thus, the locus of the CFDF detection system, according to the schematic diagram (Fig. 4), was calculated for constant scattering angle $2\theta_0=90°$, flight path lengths $A_0=3.33$ m and $B_0=1.14$ m. The tangent angle, calculated for A_0 and B_0 is represented in Figure 5.

The detection system aperture has been precisely calculated by a special program which analyze the detector element positions needed for the fulfillment of the time focusing condition. Thus, the angular aperture was found [25] equal to $\Omega_D=5.1\text{x}10^{-2}$ steradians.

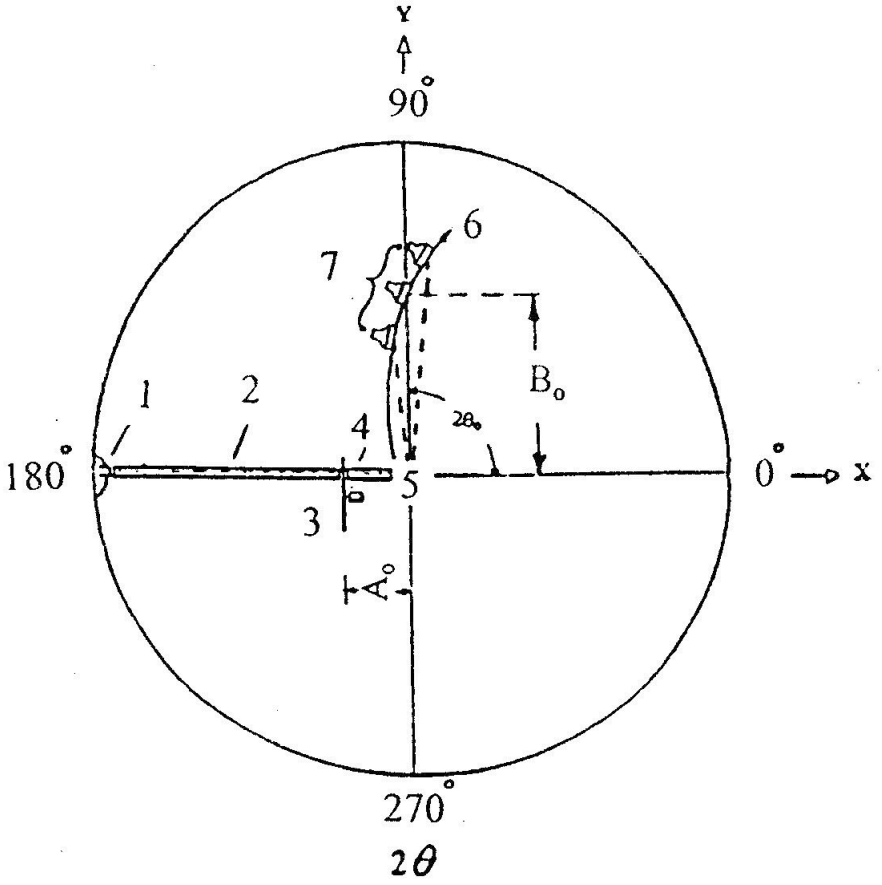

Fig. 4: The locus of constant time of arrival for the detection system.

A neutron diffraction measurement was carried out for a standard diamond powder sample with the CFDF. The diamond sample was contained in a cylindrical Al foil (5 mm in diameter and 85 mm in height) and the Fourier chopper was rotating at 8000 rpm. Figure 6 shows the diffraction pattern of the powdered diamond measured within 30 minutes at room temperature.

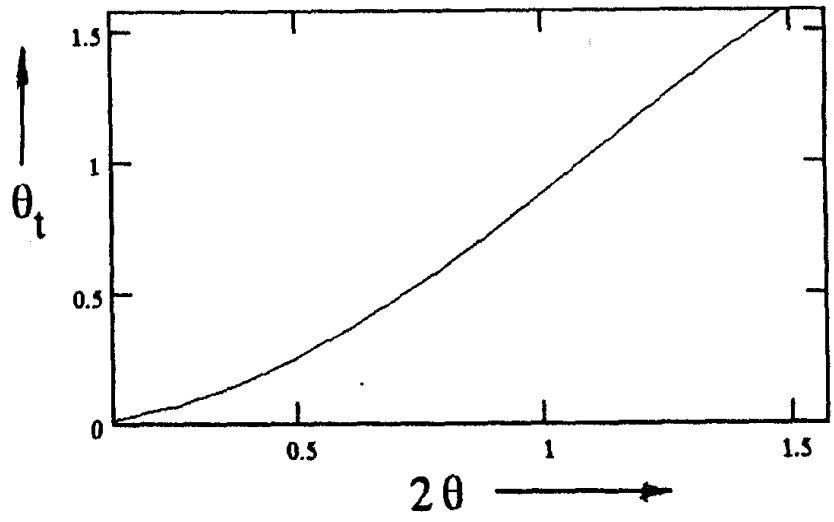

Fig. 5: The dependency between the tangent angle θ_t and the scattering angle 2θ.

It is noticeable from Fig. 6, that good separation between the peaks (i.e., good resolution) and high counting rate could be achieved within short measuring time.

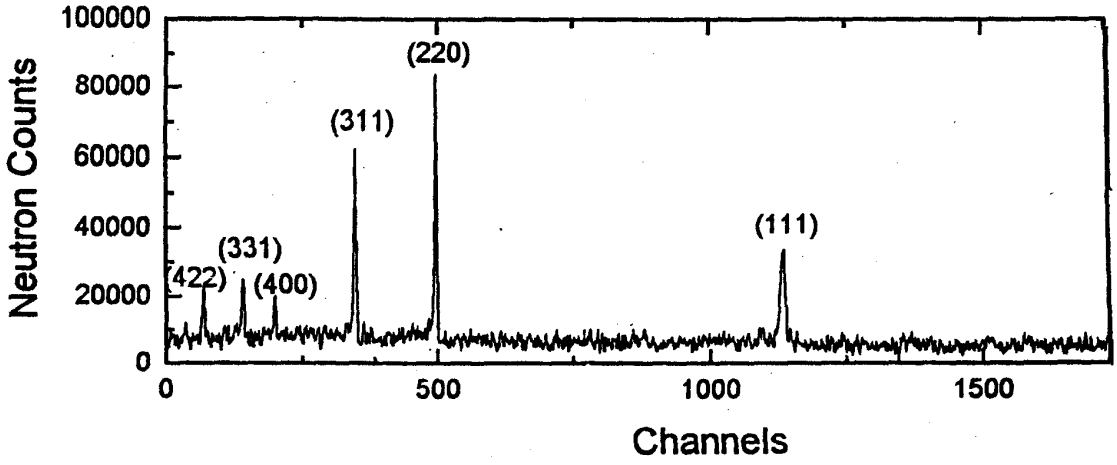

Fig. 6: The diffraction pattern obtained for a diamond powder sample.

The Gaussian fitting model was used to determine the diamond peaks positions and their FWHM (Δ_{Dhkl}). Figure 7 shows an example for one of the peaks, fitted by the Gaussian model.

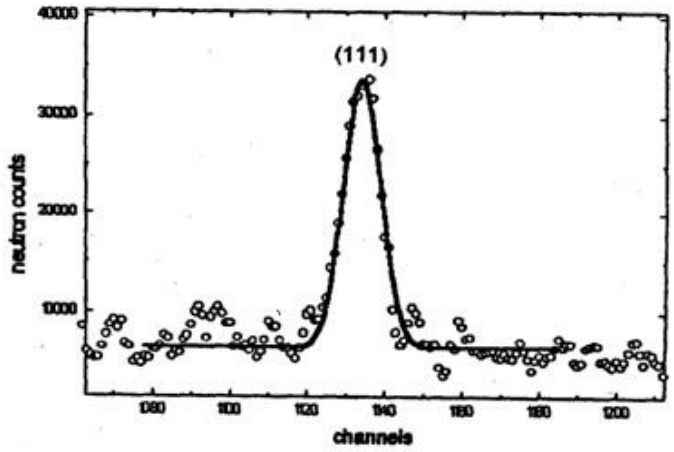

Fig. 7: The diamond (111) peak as fitted by a Gaussian model.

Consequently, it has been concluded that the CFDF with the adopted geometry could be suitable for measurements required for solving condensed matter problems. The diffraction pattern, which was measured using the CFDF for Al powder sample, is displayed in Figure 8, as well as Buras one [26] obtained by using a conventional TOF method.

It is noticeable from Figure 8 that the quality of the presently measured diffraction pattern, with regard to resolution and intensity, is superior to that one obtained with the conventional method. Figure 9 represents the diffraction pattern obtained for the Al_2O_3 powder sample along with that one obtained [22] by an analogous RTOF diffractometer (Mini-Sfinks, Russia), whose detector is set at a backward scattering angle (155°), for crystal structure investigations.

Nevertheless, the quality of the Al_2O_3 diffraction pattern, measured with the CFDF, whose detector is set at 90^o, is almost the same as that one obtained by Mini-Sfinks [22]. This confirms the possibility of successful use of the present geometrical arrangement of the detection system at the CFDF for crystal structure investigations.

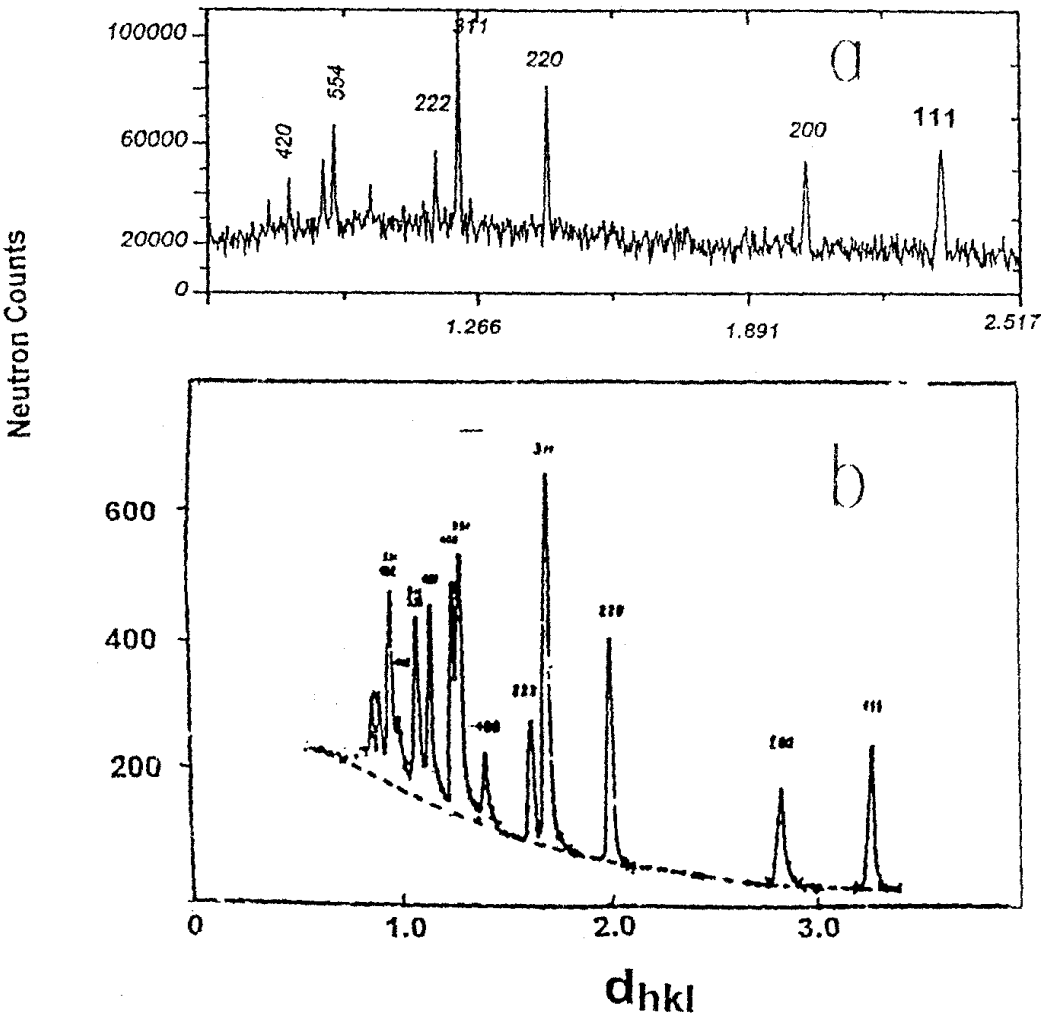

Fig. 8: The Al diffraction patterns
a) Present;
b) Previously reported [26].

2.3. On the resolution of the CFDF

The neutron diffraction measurements were performed for powder samples from aluminum oxide (Al_2O_3) and aluminum powder metal and further used for studying the behavior of the CFDF resolution. The behavior, represented in Figure 10 and deduced from the FWHM of the observed diffraction peaks, was found to be consistent with that previously deduced from measurements with different powder samples at d spacing values between 0.7 Å - 2.1 Å and scattering angle $2\theta=90°$. This makes it possible to obtain, using the CFDF, diffraction patterns which are useful for studying crystal structure and still preserving a reasonable resolution.

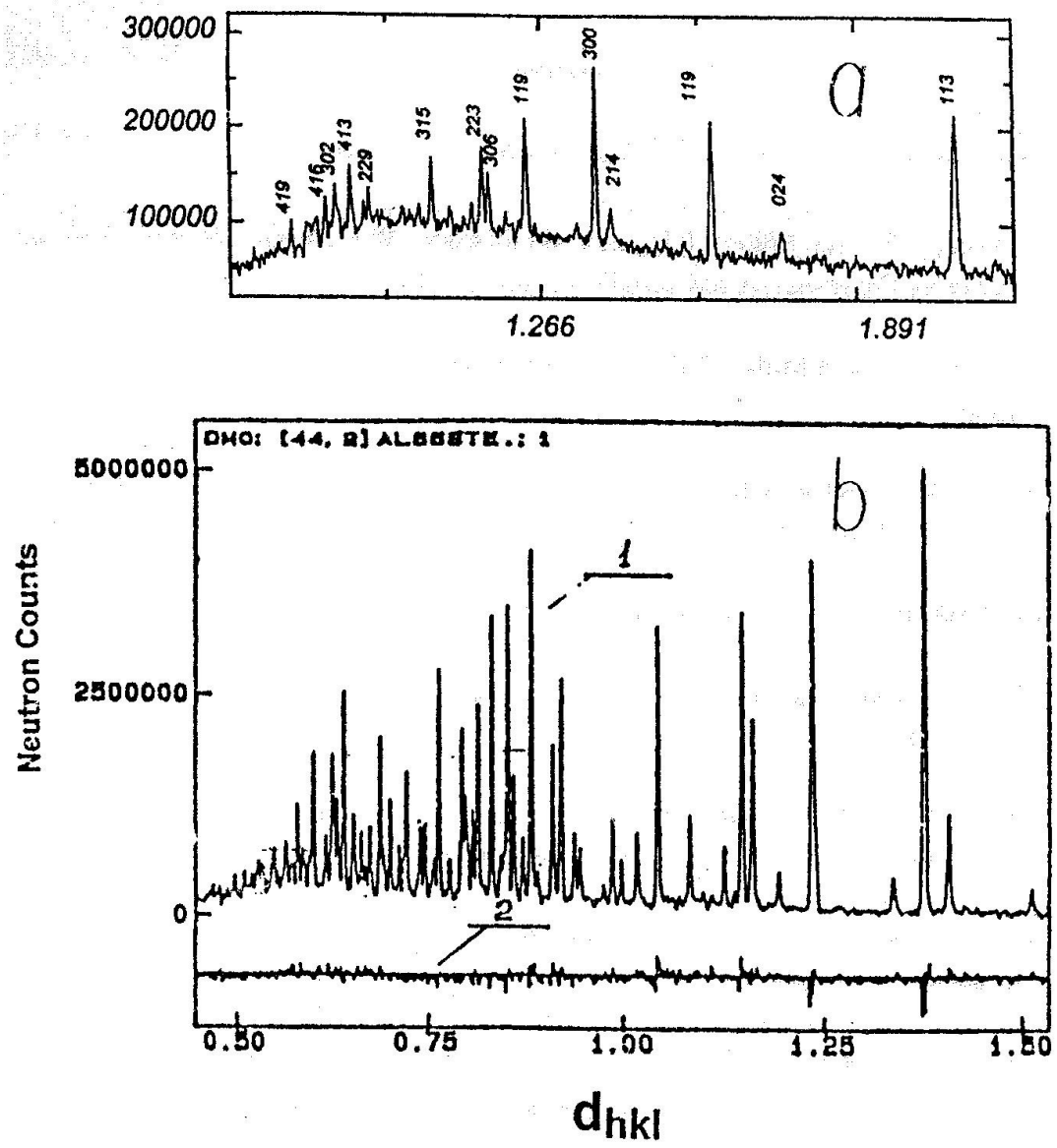

Fig. 9: The Al_2O_3 diffraction patterns
a) Present;
b) Previously reported [22].

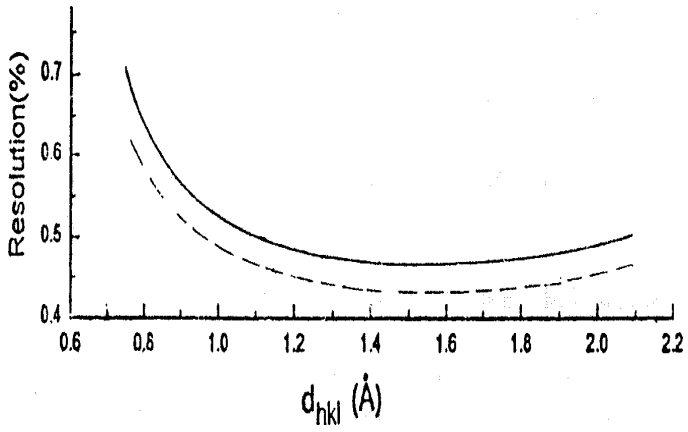

Fig. 10: The CFDF resolution:
— Present; ----- Previously reported [15].

2.4. Measurements for Stress Analysis

Preliminary measurements [27] were performed using two electrically welded iron rods and a free rod of the same dimensions. The results of measurements confirmed the adequacy of the CFDF for studying the residual stress after welding. Furthermore, the measurements using steel and copper rods [28] were performed both for electric and argon welding.

The measurements were carried out at a room temperature, under the following set-up conditions of the CFDF: the maximum rotation speed of the Fourier chopper is equal to 8000 rpm, the frequency window is Gaussian with delay time of 2048 μs, the RTOF analyzer is set at channel width of 2 μs. The diffraction patterns obtained for both steel and copper are similar to that one displayed in Figure 11.

As a result of the measurements, it was concluded [28] that:

- The CFDF could be successfully used to perform neutron diffraction measurements and for studying residual stress at considerable counting rates of the detection system in a relatively short time, thereby significantly saving the measuring time;

- The electrical welding is more adequate (for both steel and copper), than the argon one and the residual strain was found to be smaller in case of electrical welding spectra;

- However, more work still need to be performed on the industrially applicable analysis of diffraction spectra which were measured for other samples. This will help a lot both in the conclusive evaluation of the CFDF and for the additional components, which will be required for its practical use saving the reactor's operation time. Some of the mentioned measurements will be displayed later.

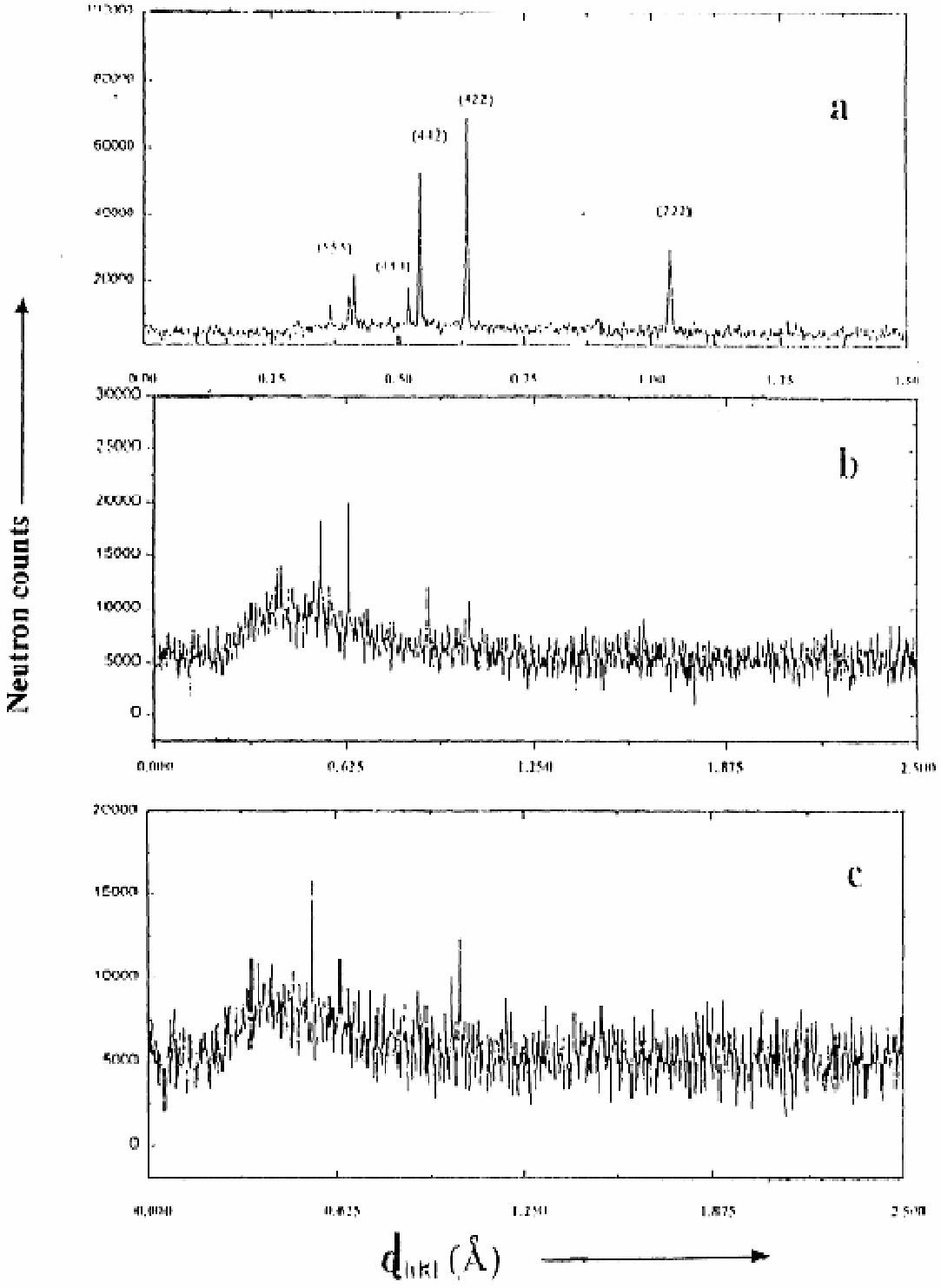

Fig. 11: The diffraction patterns of copper:
a) free sample;
b) after argon welding;
c) after electrical welding.

3. New developments of the CFDF

A new design for the CFDF reverse time of flight analyzer was introduced by Maayouf [25]. The new design applies a data acquisition system, a special interface card, and a software program installed in the computer which operates the CFDF in order to perform the required cross-correlation functions.

The first version of the interface card [30] was designed for the CFDF, as attached to the steady state ET-RR-1 reactor. Accordingly, the neutron diffraction pattern of an iron sample was measured using both the designed interface card and the attached to the CFDF RTOF analyzer (made by VTT in Finland). In comparison with the results of the Finnish made analyzer of the CFDF, the obtained spectra were found to be the same, except for the substantially higher level of noise and background. It was noticed (Fig. 12) that the noise level had been increased from about 2500 neutron counts to about 10000 neutron counts, and, consequently, the peak to background ratio of the highest peak had been reduced [31] from about 8 to about 4.

Accordingly, in order to overcome the problem of noise and background there was a need to modify the introduced design. Thus, the designed interface card was reconstructed [32] and further developed. Besides, in order to improve the performance of the new design the software program was also further enhanced.

The new data acquisition system was first implemented and tested at the high resolution Fourier diffractometer facility (HRFD) installed at the IBR-2 pulsed beam reactor of the JINR (Dubna-Russia), and the software card was also adapted for the simultaneous operation with two separate detection systems. Thus, the new approach was first tested using a Pentium 133 computer installed in parallel with the RTOF analyzer of the HRFD. The two patterns, measured for an iron sample, using the developed new approach and the Finnish made RTOF analyzer of the HRFD, are displayed in Figure 13.

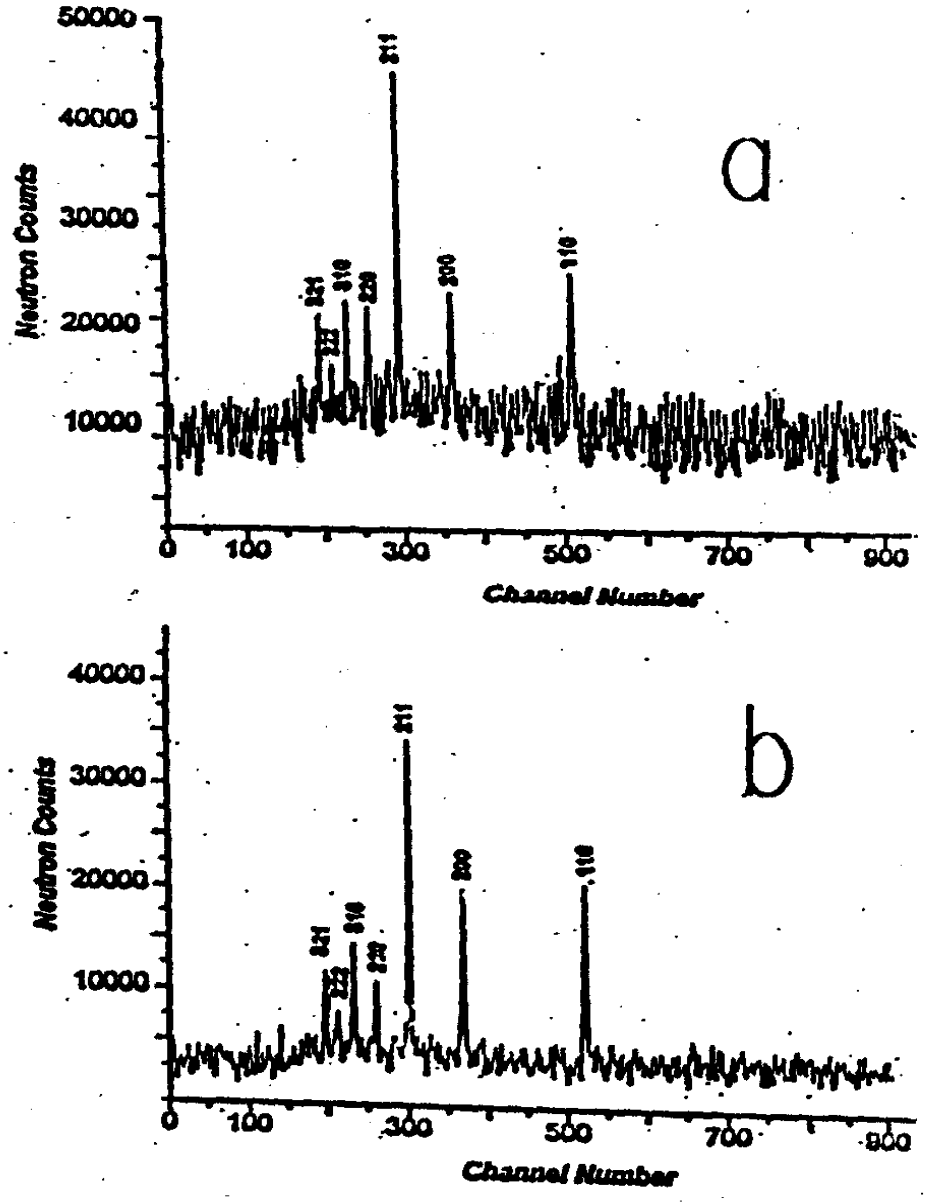

Fig. 12: The iron diffraction patterns measured using:
a) new approach analyzer;
b) CFDF analyzer.

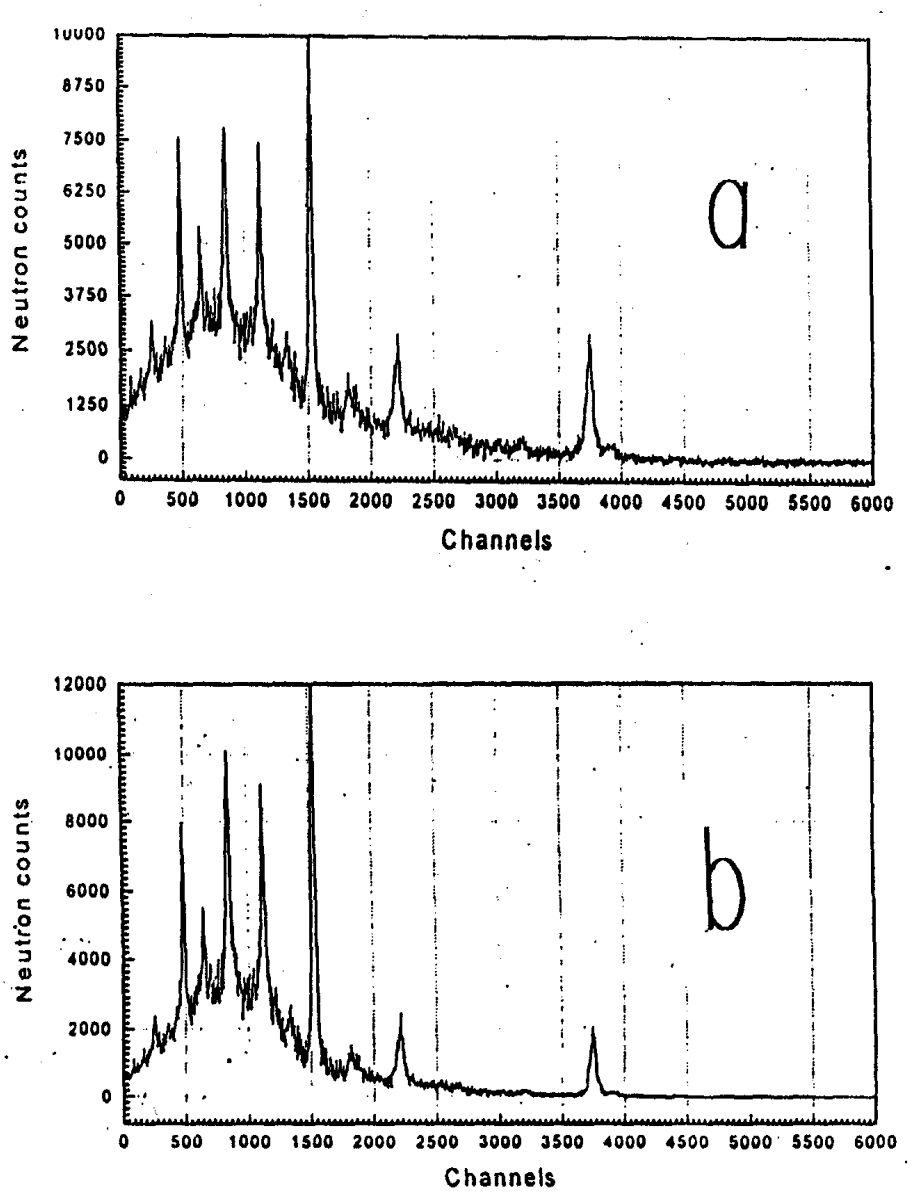

Fig. 13: The iron diffraction patterns measured using HRFD
a) Measured using new data acquisition system;
b) Measured using the RTOF analyzer.

It is noticeable that both diffraction patterns are almost the same, except for the noise level which has been increased by ~22% for the new system. This is due to the fact that the signal-to-noise ratio is usually higher in case of pulsed neutron source [14]. The two patterns obtained from the testing of the new data acquisition system at the CFDF are represented in Figure 14. Accordingly, the peak positions are the same for the two patterns. It is noticeable that both diffraction patterns are consistent, except for insignificantly bigger background and noise in the pattern obtained with the new system. The noise level has been increased from about 600 neutron counts to about 1000 neutron counts and the peak to background ratio of the strongest peak has been reduced from about 12 to about 8. This is mainly due to the limited size of the FIFO unit (2048 bytes) and the limited speed of the computer.

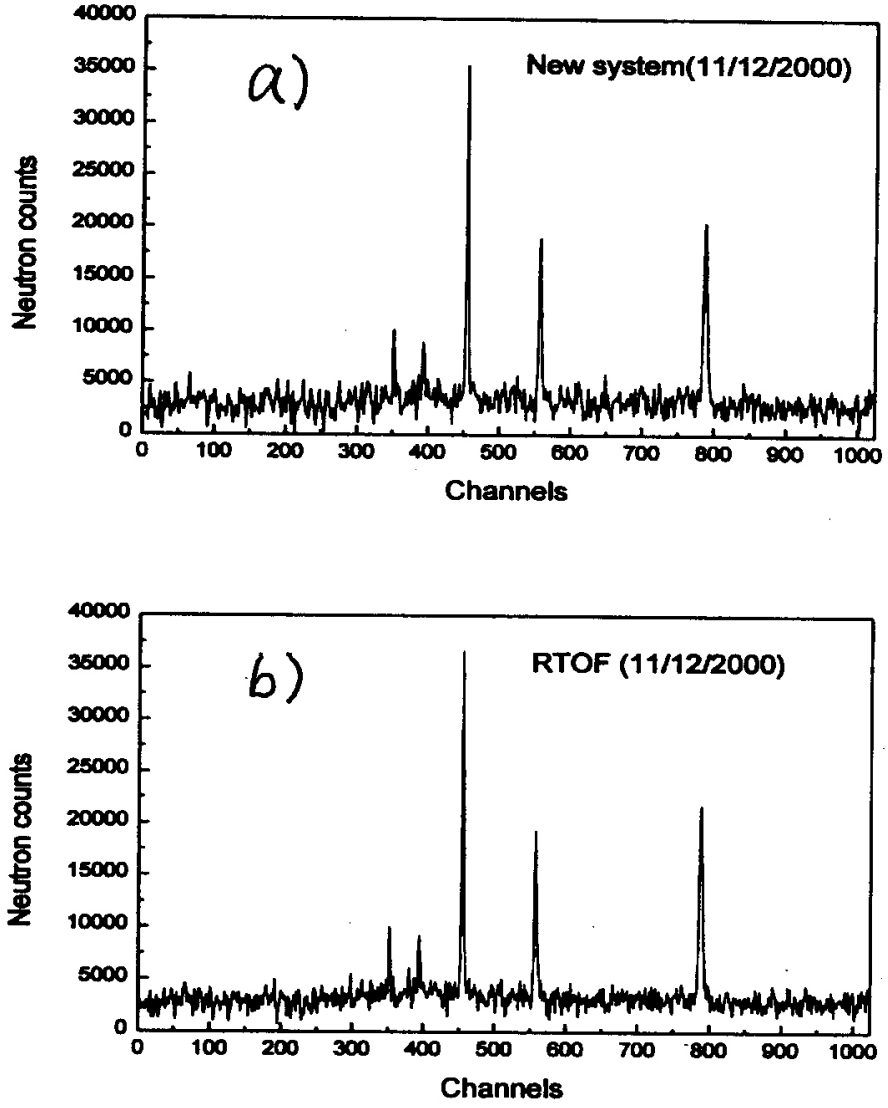

Fig. 14: The iron diffraction patterns measured using the CFDF.
a) Measured using the new data acquisition system;
b) Measured using the RTOF analyzer.

A complete development of the reverse time of flight analyzer, used with the CFDF, was worked out [33] for the registration and analysis of the neutron RTOF spectra. The block diagram of the interface board is represented in Figure 15. Accordingly, the interface board receives the neutron intensity signals coming out from the four elements of the CFDF detection system together with the pick-up signal from the Fourier chopper.

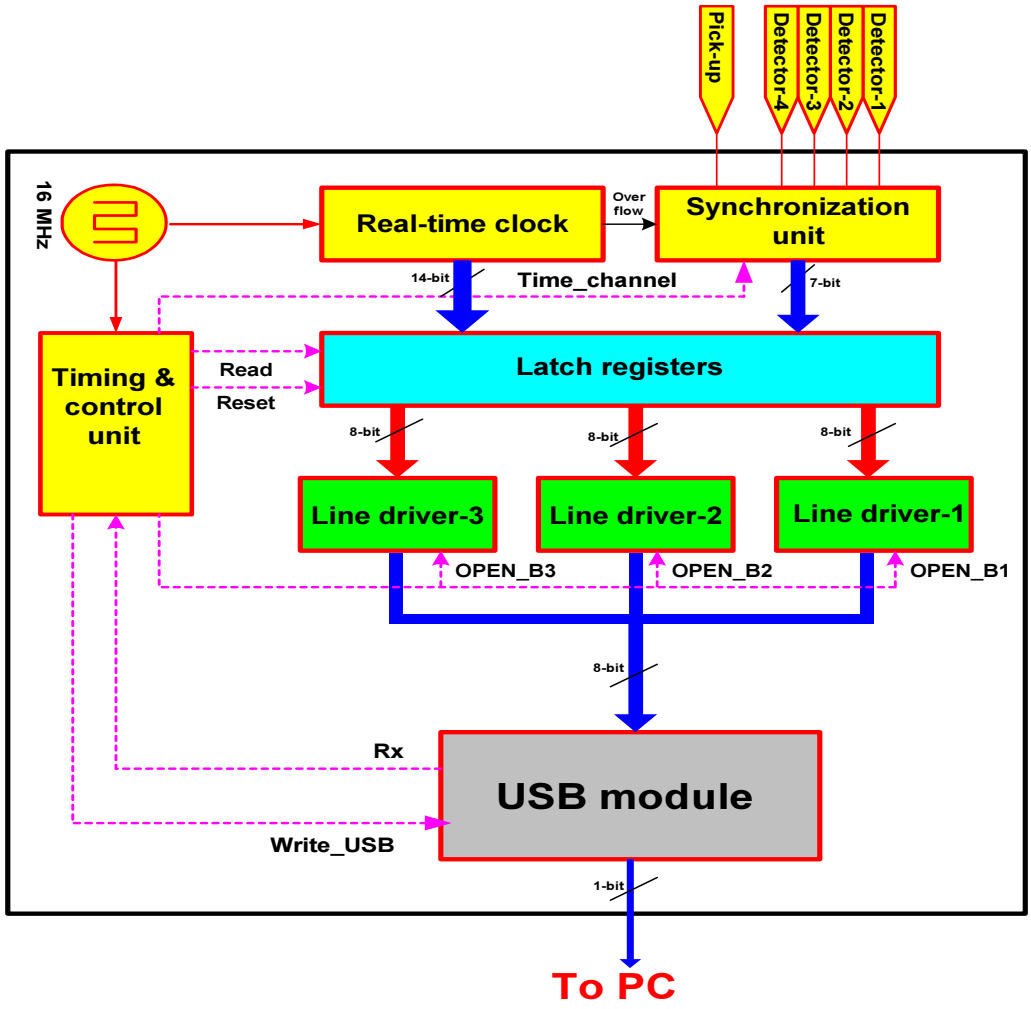

Fig. 15: The block diagram of the interface board.

The analog section of each detector's electronics (preamplifier, amplifier and discriminator) converts the detector charge pulse into a logical pulse of fixed width (~ 50 ns). The pick-up signal is generated by the chopper encoder and its frequency is proportional to the rotation speed of the chopper. The Fourier chopper consists of a rotating disk with 1024 periods, comprising one neutron absorbing and one neutron-transmitting sector of equal angular widths, as it was explained in ref [15]. Accordingly, at maximum rotation speed of 9000 rpm the pick-up frequency of the pick-up signal is = 9000 x 1024 / 60 = 153.6 kHz.

The random input pulses are synchronized with the system clock (16 MHz) in the synchronization unit. A 14-bit real time, derived with 1 MHz clock, generates the real-time of each detector or pick-up event with 1 μs resolution. With 1 μs clock tick and 14-bit counter the maximum measuring time before the clock overflow is about 16 ms. In order to allow almost infinite measuring time, the clock overflow output is passed with the collected data to the analysis software for computing the time-of-arrival of each event. A 24-bit data bus (14-bit counter, 1-bit overflow, 4-bit detectors, 1-bit pick-up event, 1-bit pick-up value and 3-bit reserved) is fed to the clocked latch register. The latch register bits corresponding to the event signals are together giving rise to a strobe pulse. This strobe pulse is used to write the contents of the latch register (24-bit frame) successively in three steps (one byte in each step) to the FIFO (8-bit width and 384 bytes in depth) of the USB module providing that the write operation is allowed at this moment (Rx signal from USB must be low). The reserved three bits are distributed as one bit for every byte of the frame to allow the program distinguishing the first, second and third bytes of the frame. The timing and control unit generates the different clock frequencies required for signals synchronization and the timing of the data transfer between the different units of the interface board.

Thus, the completed system receives the digital pulses coming out from each of the detection system's elements along with the pick-up signal from the Fourier chopper. The system's data acquisition board interfaces directly to the PC through a commercial universal serial bus (USB) module allowing asynchronous transfer of the buffered data to the software residing on the PC. The completed [33] data acquisition system (interface board and software program) was implemented and installed in one of the recent PC.

The system has been initially tested to perform the chopper pick-up autocorrelation functions, while rotating at maximum speed of 6000 rpm, according to specific frequency window. The result was found to be the same as that reported before [32] with the Finnish made RTOF analyzer. Besides, the diffraction pattern, measured for an iron sample using the completed data acquisition system, was found to be the same. The measured pattern is represented in Figure 16. The contribution of each of the four detector elements to this diffraction pattern is represented in Figure 17.

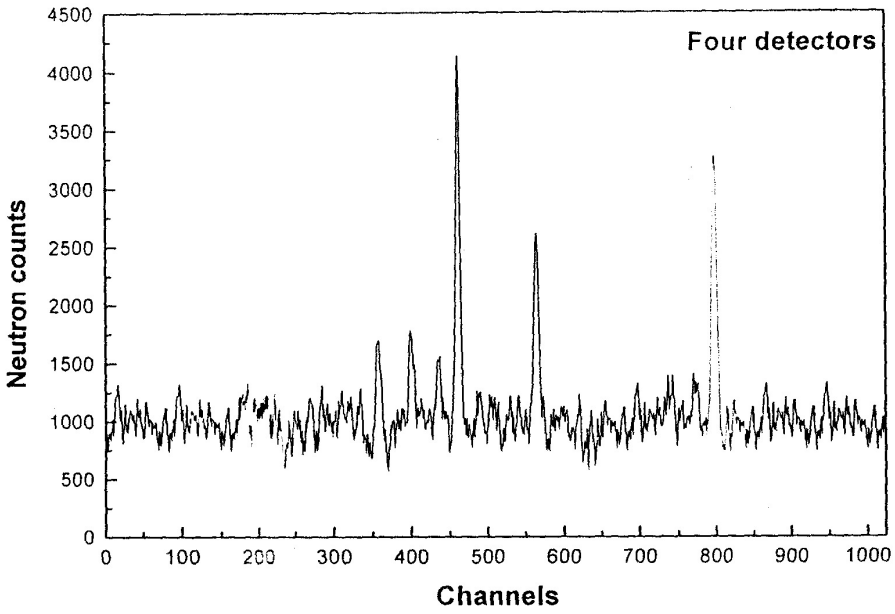

Fig. 16: The diffraction pattern measured by the USB-based data acquisition system.

It is noticeable that the pattern of the second detector element has clearer peaks and higher peak-to-background ratio (background level is ~14%) compared to the other three detector elements. The build-up of the diffraction pattern could be displayed periodically every one minute during the time of measurement.

There are big chances that the present complete development of the designed acquisition system, being worked out in its final form along with its software, will be more efficient for use at the CFDF, than the previously reported [32] substitute of the Finnish made RTOF analyzer, since it provides the on-line display of the developing diffraction pattern of the measured sample. Besides, it will allow monitoring of the efficiency of each of the detection system elements and their associated electronics.

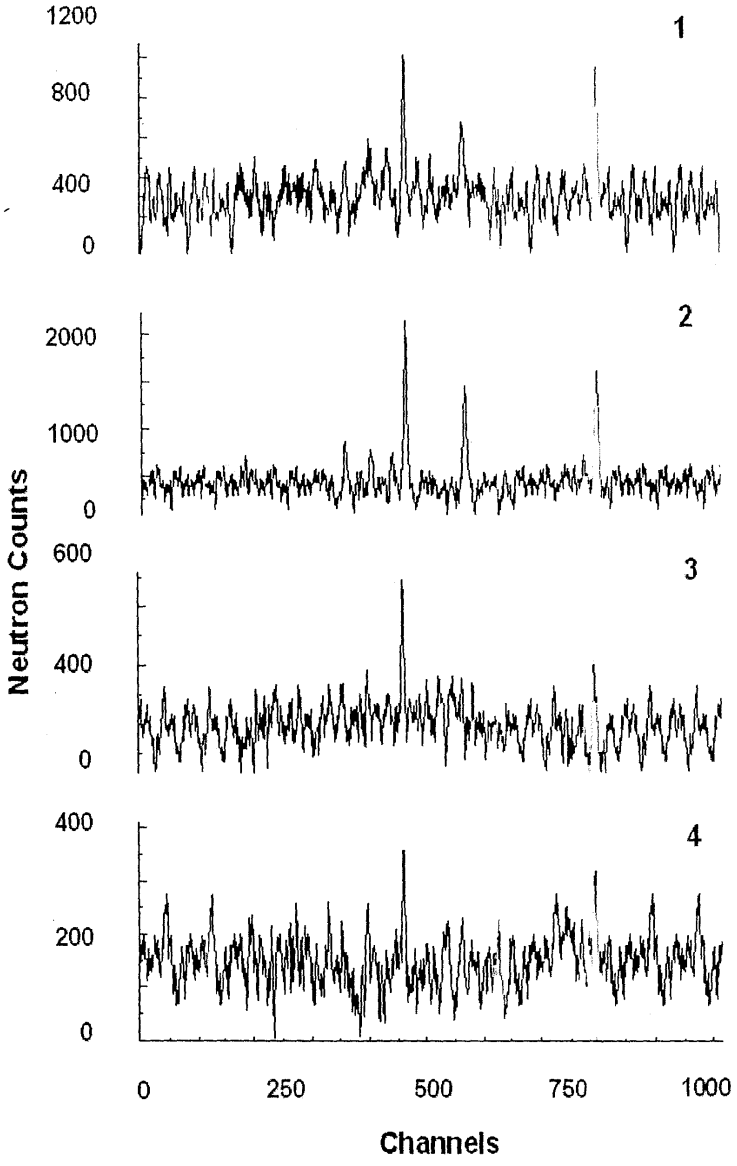

Fig. 17: The contribution of each detector to the diffraction pattern.

4. Fault Diagnostic System

A fault diagnostic system was developed for the CFDF. It consists of two levels (see Fig. 18). The first is feed-forward back-propagation neural network used for isolating the faulty part of the CFDF. The second is the rule-based expert system used for trouble shooting the faults inside the isolated faulty part.

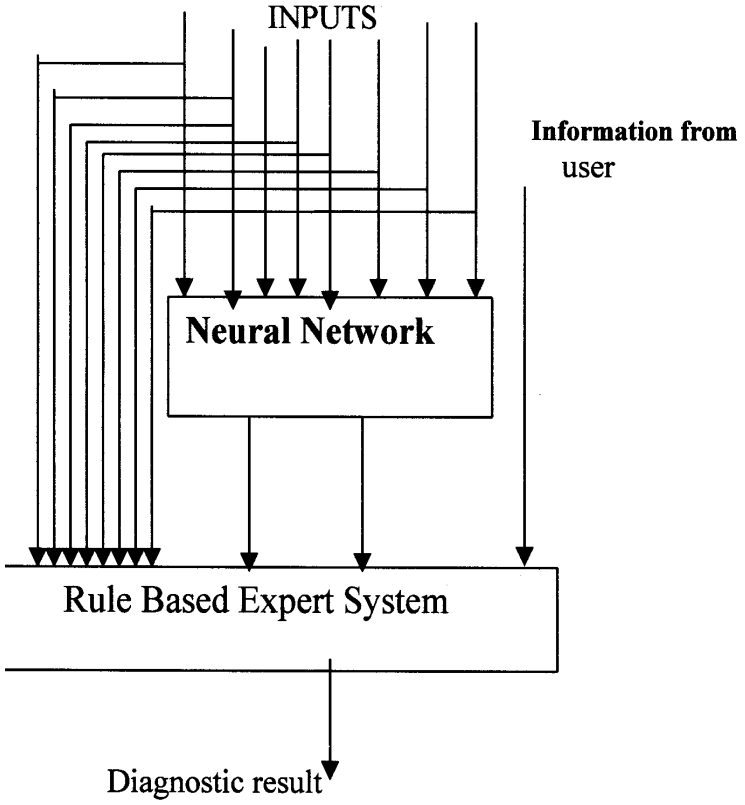

Fig. 18: Schematic diagram for the developed hybrid expert system.

The developed diagnostic system after the preliminary tests proved to be adequate and flexible when used with the CFDF. At the same time further development of the fault diagnostic system was attempted in order to include all the important parts of the CFDF. This will result with a special computer program which will be loaded into the CFDF computer. This will enable to observe any failures concerned with the CFDF components during the experimental measurements.

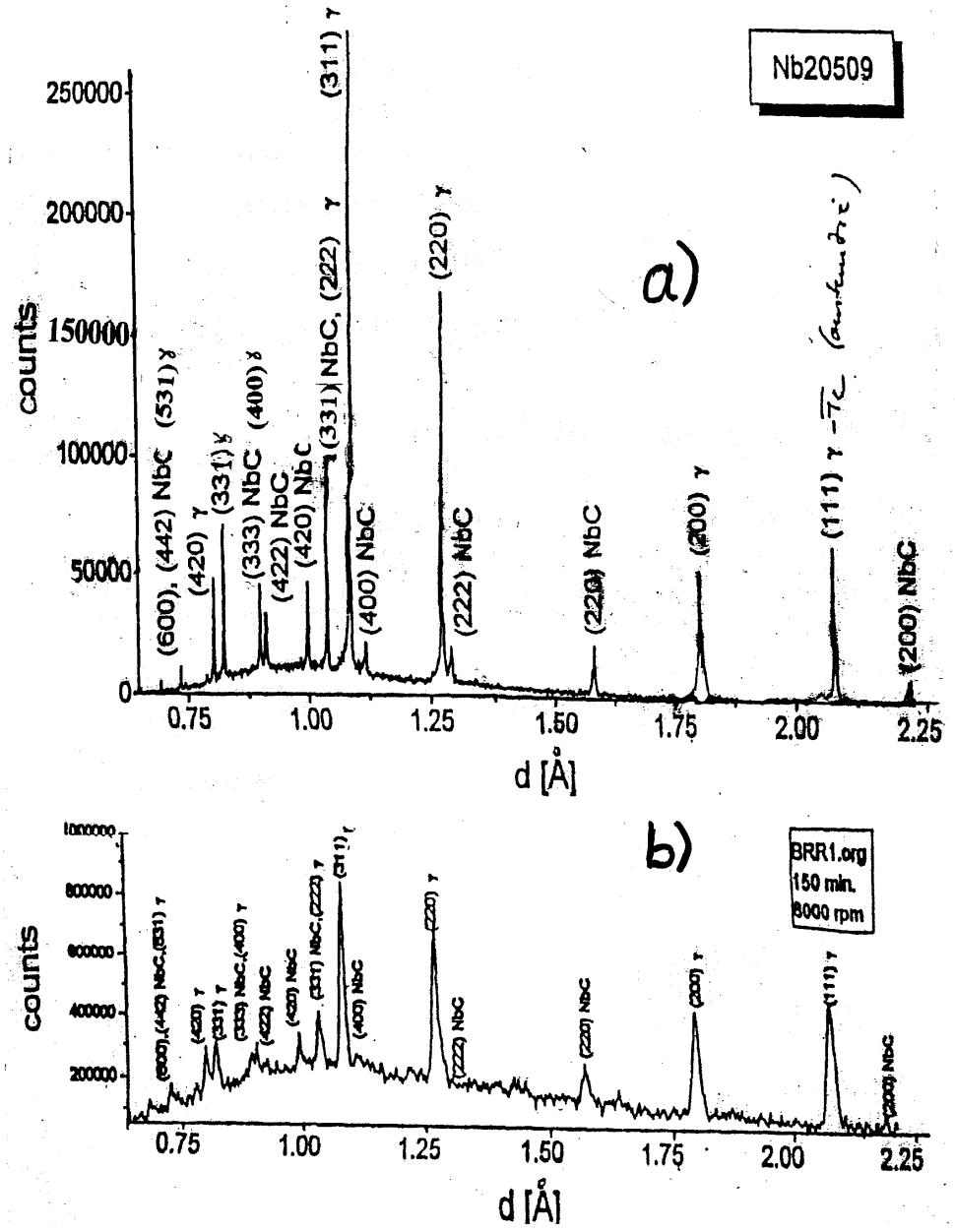

Fig. 19: The Nb diffraction patterns measured using:
a) HRFD at JINR (Dubna); b) CFDF.

Samples from Germany were analyzed with the CFDF; both for comparison with the HRFD of the JINR (Dubna) and for evaluation of the adequacy of the CFDF for studying the residual stress after welding. The results of measurements, performed with the CFDF for Nb sample (from HMI-Berlin), are compared with those which were measured before with the HRFD in Figure 19. It is noticeable that the results of the CFDF measurements are more accurate than those of the HRFD. This is more evident from the peak distributions, represented in Figure 20, since they follow well the Gaussian distributions given in the same figure; which isn't the case for the HRFD pattern.

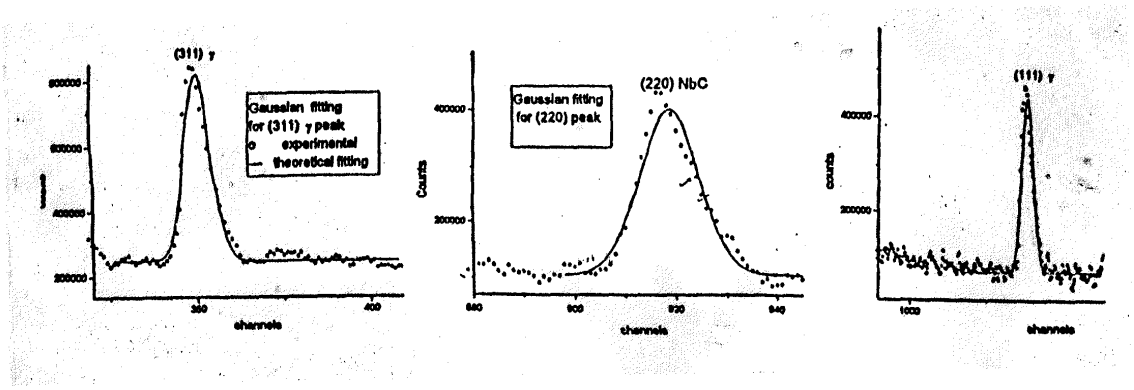

Fig. 20: Gaussian distributions at different peak levels.

The neutron diffraction spectra, measured when scanning another sample from GKSS (Germany), are represented in Figure 21. The sample itself is two welded bars of Aluminum; which could be used in aviation industry. Accordingly, the sample was moved, at the sample position, across the neutron beam of the CFDF. The neutron diffraction spectra measured at each position, are shown in Figure 21. Moreover, the sample was inverted and rescanned at the same positions, resulting with another five spectra similar to those obtained during the other scanning. This makes it possible to study the residual stress after welding and to decide about the adequacy of the welding itself.

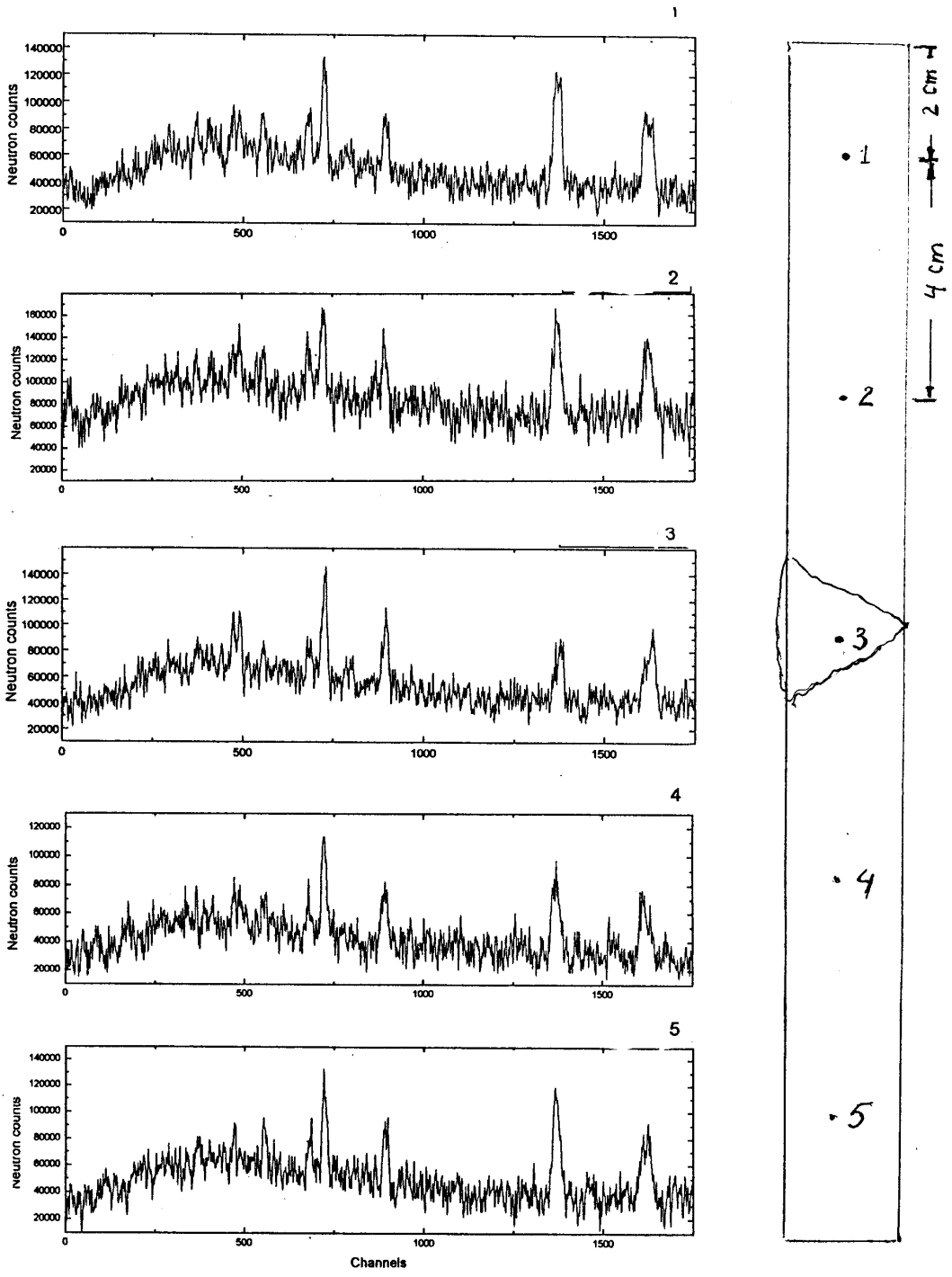

Fig. 21: The spectra measured during the scanning of the GKSS sample.

5. The development of Plastic Neutron Mirrors

Various types of neutron optical elements, such as neutron guides, are constructed from mirrors. The latter are often made of highly polished glass plates coated with a layer of a material whose scattering length is high. For example, it could be natural nickel or ^{58}Ni as in the case of the neutron guide system of the CFDF. The geometrical considerations of the neutron optical elements could require the use of a light and flexible material, as a substrate of the Ni coating; such as Plexiglas. Consequently, it was found important to study the neutron reflectivity from nickel films coated on such type of substrate; since this should significantly help to build a neutron guide system for the ET-RR-2 reactor in Egypt; due to its limited number of horizontal experimental channels in comparison with the ET-RR-1 reactor.

Such measurements were started in the beginning of 90's. Accordingly, measurements were performed by Maayouf *et al.* [35-38] for NiCr (80% Ni, 20%Cr), ^{58}Ni and natural Ni films coated on different types of Plexiglas (German made). Despite the fact that most of the measured coatings gave almost 100% reflectivity, more measurements were still required for the conclusive test of the validity of Plexiglas as a substitute of glass in mirror manufacturing; especially when considering the deterioration of the mirror coating over the years. Another question includes the surface roughness of the substrate and the type of coating. The goal is to find out an optimum of the parameters for neutron mirror devices; designed for use at research reactors.

The present report contains more measurements performed for nickel mirrors on different types of commercially available Plexiglas. The main goals of the extra measurements are to test conclusively the validity of the nickel mirrors as a substitute of glass, and to find out their deterioration rate.

5.1. Experimental details

Three sets of reflectivity measurements using different neutron reflectometers were performed a few years ago. The first two sets of reflectivity measurements were performed using two different monochromatic neutron reflectometers described in details by Ebisawa and Maayouf [40, 41]. The first set was performed for four Ni mirrors on different Plexiglas substrates. While two of the mirrors were with ^{58}Ni coatings (150 nm thick), the other two had 700 nm thick NiCr coatings (80% Ni, 20%).

The four Plexiglas mirrors were prepared in 1991 and neutron reflectivity measurements were performed in 1991 and 1993 respectively for one of the NiCr mirrors and the Ni one on Makrolon Polykarbonat substrate using the time of flight reflectometer of St. Petersburg Nuclear Physics Institute [35, 36]. Regardless, the neutron reflectivity of both mirrors was measured again in order to check the changing in the quality of such type of mirrors over several years. Four years later another measurements were performed, using the (C3-1-2) reflectometer installed at a cold neutron guide tube of JRR-3M reactor of JAERI (Japan) and incident neutrons with a long wavelength (12.6 Å), with the glancing angle θ which was varied between 0.5°- 2.9°, covering values (θ/λ) respectively between 0.0007 and 0.004 rad/Å. More details about the reflectometer could be found in Ebisawa work [40].

The second set of measurements was carried out for two NiCr films on Plexiglas and one ^{58}Ni film (150 nm thick) coated on a glass substrate. The two Plexiglas mirrors were prepared in 1991 and are coated with 700 nm thick layers of NiCr (80% Ni, 20% Cr). While one of the two mirrors was on 1 mm thick Plexiglas, the other one was on a rather thinner foil (100 μm thick). The reflectivity of the two Plexiglas mirrors was also measured using the (C3-l-2) reflectometer of the JRR-3M reactor (Japan); mentioned before. The reflectivity of the ^{58}Ni glass mirror was measured using the pyrolytic-graphite reflectometer, described by Maayouf [39], with neutrons of wavelength 4.3 Å.

The third set of measurements was performed using the D17 reflectometer, at ILL (France), working at the time-of-flight mode. The measurements were performed for two Ni mirrors. While one of them was a ^{58}Ni film (150 nm thick) coated on boron loaded glass (1 cm thick), the other one was a natural

Ni (99.9%) film of 700 nm thickness , coated on PMMA plastic substrate (2.5 mm thick). The latter mirror was prepared in 1991 and measured before.

5.2. Results and discussion

The dependencies between the neutron reflectivity and θ/λ (rad/Å), deduced from the first set of the measurements for the ^{58}Ni mirrors, are displayed in Figure 22. a previous measurement [36] was performed five years before for one of them and yielded then the critical value of $\theta/\lambda = 19.1 \times 10^{-4}$ rad/Å. This critical value is consistent with the value 18.7×10^{-4} rad/Å, deduced from the presented measurements for both types of Plexiglas. This is in favor of the quality of the mirrors as they were prepared seven years before the present measurements.

The neutron reflectivity behaviors deduced from the first set of the present measurements for the two NiCr mirrors are presented in Figure 23. The previous measurement [35], which was performed for the same mirror using a neutron beam spectrum incident on the mirror at a fixed glancing angle θ six years before (Fig. 23b), is represented in Figure 23a. All the reflectivity behaviors (Fig. 23) are rather similar: yielding reflectivity values over 90% at values of θ/λ below 14×10^{-4} rad/Å. Maxima are also observed (see Fig. 23) in the reflectivity behaviors at values of θ/λ below 20×10^{-4} rad/Å.

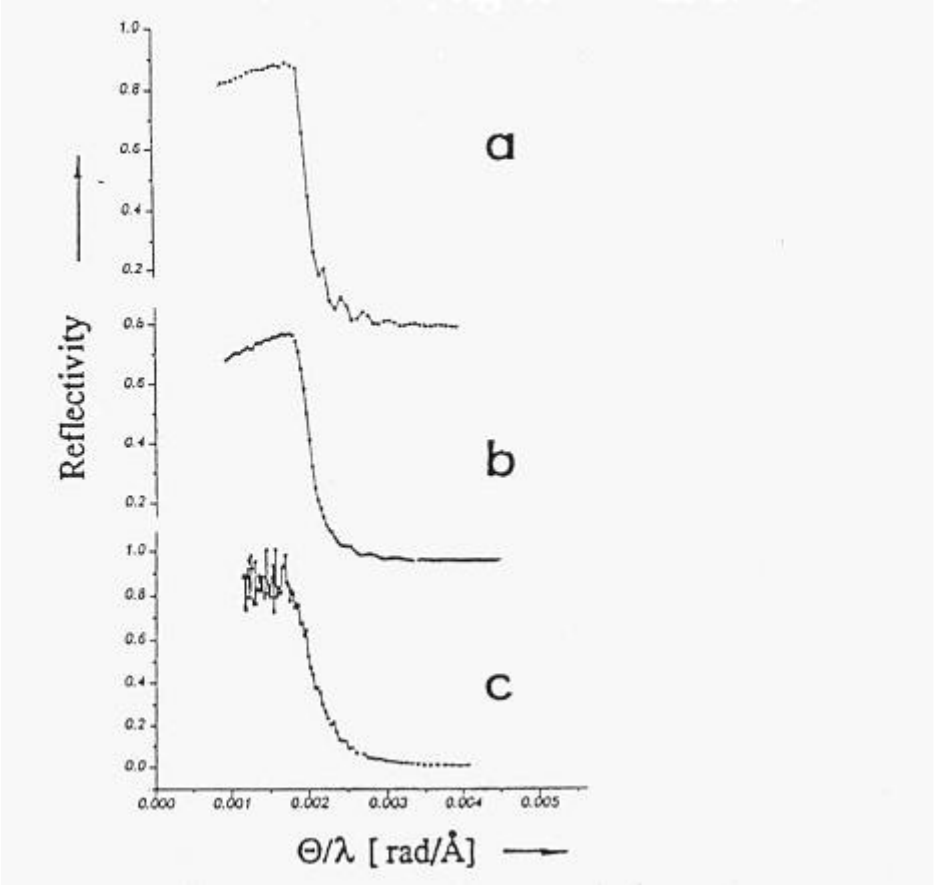

Fig. 22: Neutron reflectivities of ^{58}Ni Plexiglas mirrors
a) PMMA Plexiglas substrate;
b) and c) respectively for present and previous
measurements of Plexiglas Makrolon Polykarbonat substrate.

It was confirmed from theoretical calculations [35] and further measurements, with ^{58}Ni and natural Ni coatings that these maxima are due to a multilayer system. The latter could have been developed during the NiCr coating process, possibly, because chromium evaporates at a temperature considerably lower than that of nickel [44]. Moreover, such multilayer system was found to be characteristic for the NiCr coatings [40]. Regardless, the presented measurements with NiCr coatings

proved to be in favor of the quality of the Plexiglas mirrors, since it does not deteriorate throughout several years after preparation.

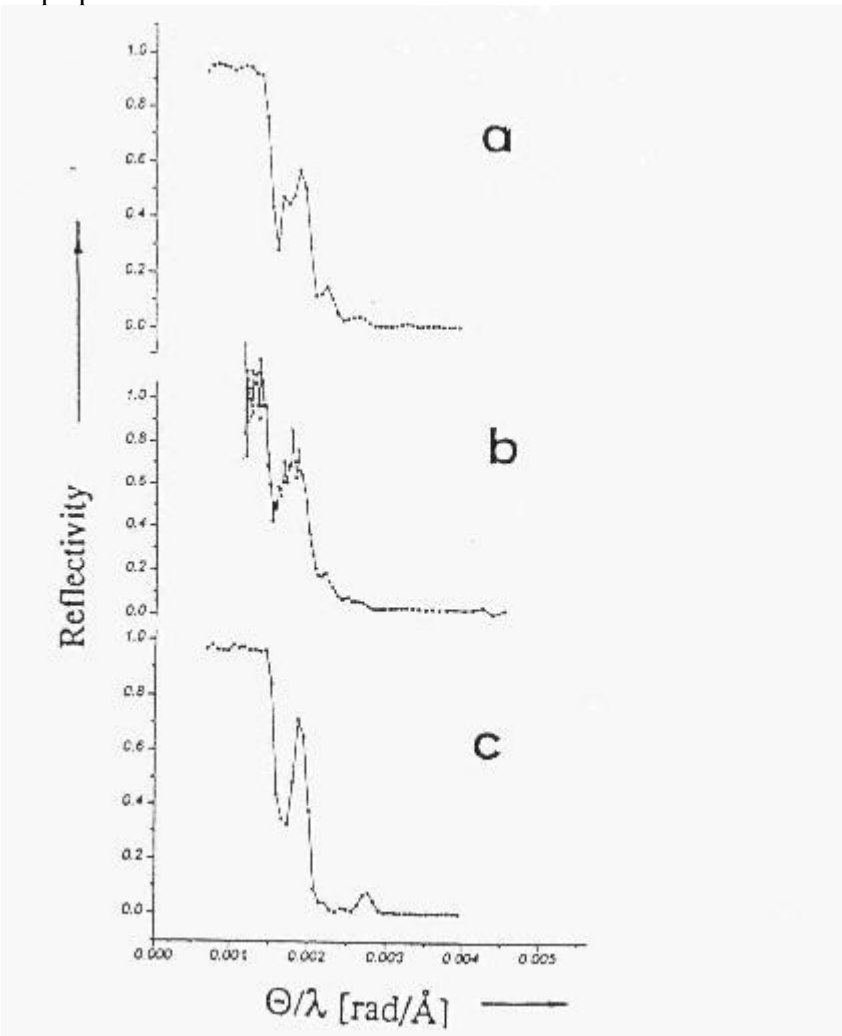

Fig. 23: Neutron reflectivities of NiCr Plexiglas mirrors.
a) and b) Respectively, for present and previous measurements of the same mirrors;
c) New PMMA Plexiglas mirror.

The neutron reflectivities reflectiviness, deduced from the second set of the present measurements for the NiCr mirrors, are displayed in Figure 24 along with previous measurements [36, 41] performed for NiCr coatings on different Plexiglas substrates. The ref1ectivity behaviors of the present NiCr mirrors are much the same as the previously measured ones; yielding the highest reflectivity at values of θ/λ below 14×10^{-4} rad/Å. The present measurements are also in favor of the quality of the mirrors.

The neutron reflectivity behaviors of the ^{58}Ni glass mirror, deduced from the presented measurements, is displayed in Figure 25 along with the results of measurements performed for ^{58}Ni and a natural Ni mirrors on Plexiglas substrates. One can notice that the reflectivity behavior of the Ni mirror (Fig. 25b) is similar to that of the ^{58}Ni mirror except for the critical value (16×10^{-4} rad/Å) of θ/λ which is lower than the value 19×10^{-4} rad/Å of the Ni mirror on glass substrate.

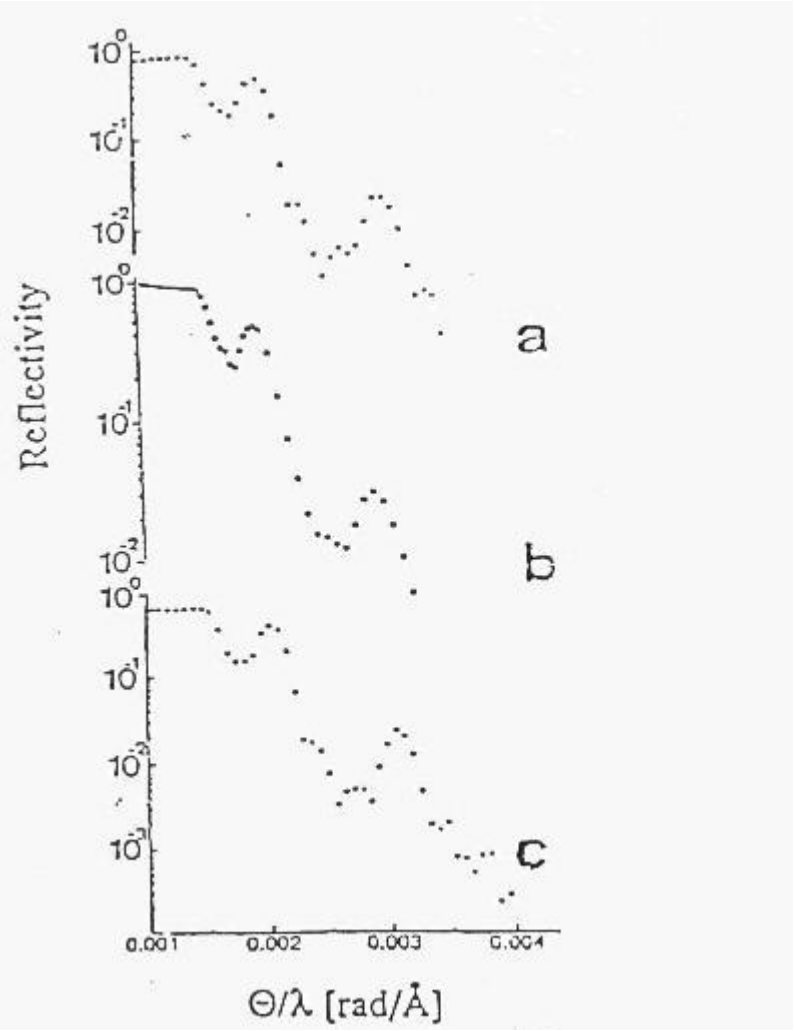

Fig. 24: Neutron reflectivities of NiCr mirrors.
a) NiCr Polycarbonate Plexiglas mirror [36];
b) Present measurement for the same mirror;
c) Present measurement for the NiCr mirror on Kalle Hostaphan foil.

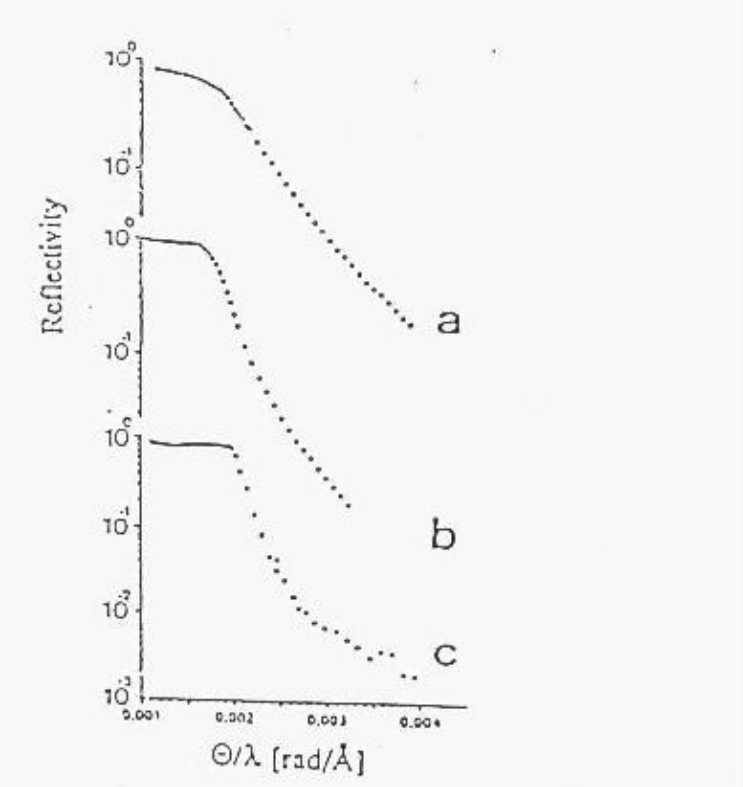

Fig. 25: Neutron reflectivities of 58Ni coated mirrors.
a) ^{58}Ni mirror on PMMA Plexiglas [41];
b) Ni mirror on PMMA Plexiglas [41];
c) Present ^{58}Ni mirror on glass substrate.

The neutron reflectivities, deduced from the presented measurements of ^{58}Ni and Ni mirrors, using the D17 reflectometer at ILL, are displayed in Figure 26. The reflectivity behavior of the Ni mirror is similar to that of the ^{58}Ni mirror except for the critical values of the θ/λ.

The critical value of and $\theta/\lambda=19X10^{-4}$ rad/Å, deduced from the present measurements for ^{58}Ni coating on glass is higher than the value 16.6 rad/Å deduced for the Ni coating on Plexiglas. This is mainly due to the fact that the scattering length of Ni is low compared to that of ^{58}Ni. Regardless, the present values of θ/λ are consistent with the value mentioned before for the reflectivity curves (b and c) displayed in Figure 25. They are exactly the same as the present ones. Such consistency between Ni and ^{58}Ni mirrors is in favor of using Plexiglas substrates instead of glass ones. Besides, the quality of the Plexiglas mirror can last for several years without deterioration.

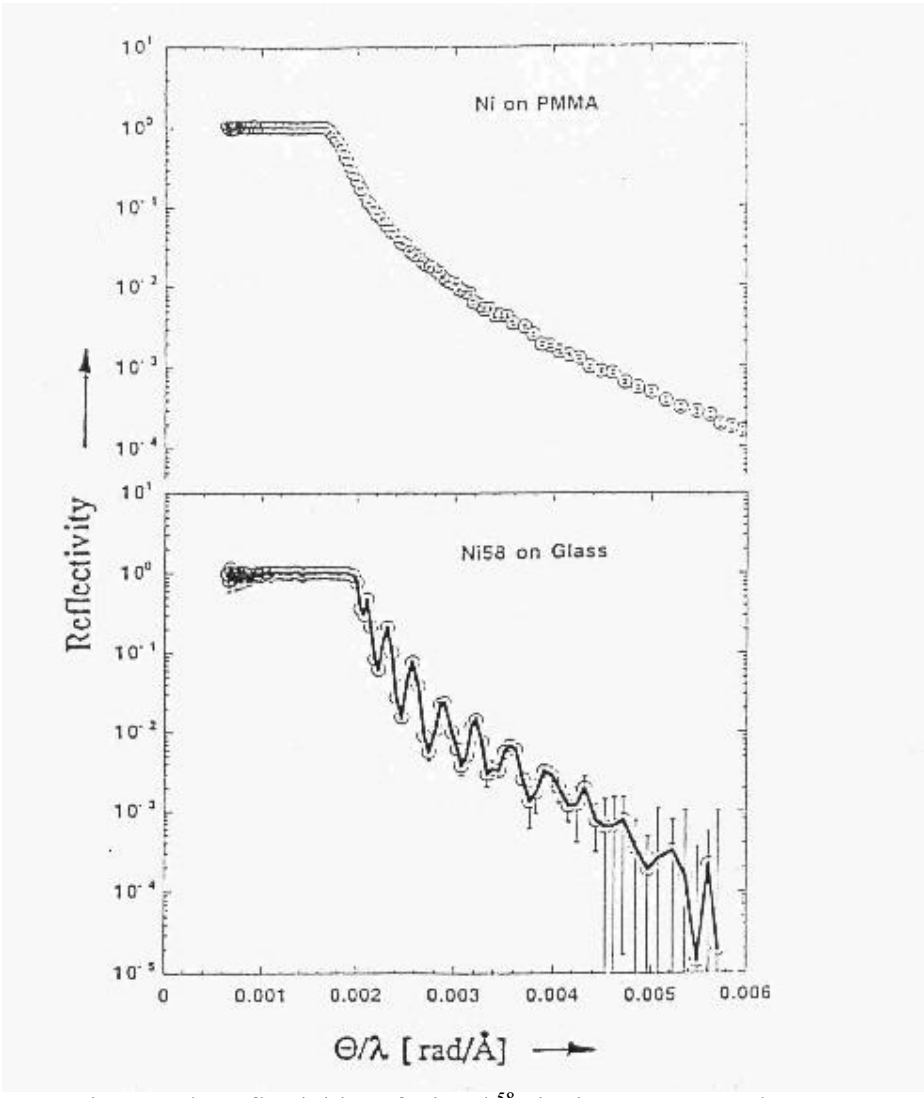

Fig. 26: The reflectivities of Ni and ^{58}Ni mirrors, measured at ILL.

It is concluded that the commercially available types of Plexiglas, such as PMMA and Makrolon Polycarbonate, could successfully replace glass as a substrate for Ni-coated mirrors [42, 43]. It offers almost the same reflectivity behavior with ^{58}Ni coating on glass mirrors and the quality of the Ni coating can last for several years without deterioration. It is also possible to use neutron mirrors on very thin Plexiglas foils for the construction of neutron optical devices.

6. Conclusions

- The CFDF can be successfully used for high resolution measurements at high count rate of the detector system; significantly saving the measuring time.

- The luminosity of the CFDF makes it possible to obtain neutron diffraction patterns at scattering angle $2\theta = 90°$ and d-spacing values between 0.7 Å – 2.5 Å with 0.45 % resolution.

- The further expansion of the CFDF for measurements at 90° scattering angle, with two detector banks at opposite sides of the incident beam, will allow for the significant decrease of the measuring time, required for the determination of the residual stresses as well as the phase analysis of polycrystalline materials. The latter can be widely made use of at steel and other metals industry.

- The neutron mirrors on Plexiglas substrates are useful for the design of a neutron guide system, essentially required for the ET-RR-2 research reactor due to its very limited number of channels.

7. Acknowledgements

- The cooperation of the IAEA staff, Drs A. Boussaha, M. Putineanu & D. Ridikas is deeply acknowledged with thanks.

- Thanks to Prof. V.G. Kadashevsky and Prof. V.L. Aksenov (JINR, Dubna, Russia) for their willing cooperation.

- The cooperation of the ET-RR-1 reactor operation group and the members of Condensed Matter Research Group (Reactor physics Dept., NRC, Egyptian Atomic Energy Authority) is deeply acknowledged with thanks.

- Thanks to reflectometry group of the PNPI (St. Petersburg, Russia) for their cooperation during neutron reflectivity measurements and for the mirrors on plastic substrates.

- The author is deeply grateful to Dr. T. Ebisawa for his willing assistance during the reflectivity assessments at JAERI (Japan).

- Dr. T. Krist (HMI, Berlin) and Prof. H.G. Priesmeyer (Kiel University, Germany), for their valuable assistances whenever it was required during the reflectivity measurements in Germany.

- The assistance of Drs. J. Zaccai, G. Fragnetto and R. Cubitt for performing the reflectivity measurements, using the D17 reflectometer at ILL (France) is deeply acknowledged with thanks.

8. References

[1] Maayouf, R.M.A., *et al.,* Report GKSS 91/E/65, Geesthacht, Germany (1991).

[2] Priesmeyer, H.G., Schroder, J., Materials Research Society (Symp.) Mat. Res. Soc. 166 (1990) 299-304.

[3] Hiismaki, P., *et al.,* Nucl. Inst. Meth. 126 (1975) 435-443.

[4] Poyry, H., *et al.*, Nucl. Inst. Meth. 126 (1975) 421-433.

[5] Poyry, H. Nucl. Inst. Meth. 156 (1978) 499-52.

[6] Maayouf, R.M.A., Tiitta, A.T., Hiismaki, P. "The RTOF Neutron Diffraction Facility at the ET-RR-1 Reactor", Report VTT Reactor Laboratory, Espoo, Finland (1990).

[7] Maayouf, R.M.A., *et al.,* VTT Research Notes 1425, Espoo, Technical Research Centre of Finland (1992).

[8] Maayouf, R.M.A., Tiitta, A.T., VTT Research Notes 1502, Espoo, Technical Research Centre of Finland (1993).

[9] Maayouf, R.M.A., Hiismaki, P.E., Tiitta, A.T., "The Multipurpose Fourier Diffractometer at the ET-RR-1 Reactor", Report VTT Reactor Laboratory, Espoo, Technical Research Centre of Finland (1993).

[10] Maayouf, R.M.A., Tiitta, A.T., Hiismaki, P.E., VTT Research Notes 1699, Espoo, Technical Research Centre of Finland (1995).

[11] Maayouf, R.M.A., Enhancement of Research Reactor Utilization (Int. Seminar, Bhabha Atomic Research Centre, Bombay, India, 11-15 March 1996) IAEA –SR-198/15 (1996).

[12] Trounov, V.A., Mini Sfinks M. "Diffractometer at Gatchina Reactor", ICANS-XIII (Conf. PSI, Switzerland, 11-14 October 1995) (1995).

[13] Schroder, J., *et al.,* Neutron Research 2, 4 (1994)129-141.

[14] Aksenov, V. I., *et al*., Neutron Research 5 (1997) 181-200.

[15] Maayouf, R.M.A., *et al.,* IAEA Report, INDC (EGY-007), Vienna, May 1997 (1997).

[16] Maayouf, R.M.A., *et al.,* Nucl. Inst. Meth. Phys. Res. Sect. A 398 (1997) 295-302.

[17] Maayouf, R.M.A., *et al.,* Neutron Research 597 (1997) 1-15.

[18] Maayouf, R.M.A., *et al.,* Egypt. J. Phys. 29 (1998) 125-33.

[19] Maayouf, R.M.A., *et al*., Egypt. J. Phys. 30 (1999) 199-206.

[20] Hashem, E.M., *et al*., ARE/AEA Rep., Cairo, Egypt (1996).

[21] Hamouda, I.F., *et al*., 9th Arab. Science Conference (Conf.) Bagdad (1966).

[22] Trunov, V.A., *et al*., LNPI Report 1266, USSR Academy of Sciences, Leningrad (1987).

[23] Maayouf, R.M.A., *et al*., J. Phys. Soc. Jpn., Suppl. A65 (1996) 238-240.

[24] Carpenter, J.M., Nucl. Inst. Meth. 47 (1967) 179.

[25] Maayouf, R.M.A., *et al*., Egypt. J. Phys. 29 (1998) 103-114.

[26] Buras, R., Report, INR N0 744/II/PS, Warsaw, August 1966 (1966).

[27] Maayouf, R.M.A., *et al.,* Egypt. J. Phys. 30 (1999) 191-199.

[28] Maayouf, R.M.A., *et al.,* Nuclear Science and Applications (Proc. Int. Conf., Sharm Al-Sheikh, Egypt, November 2007 (2007).

[29] El-Shaer, Y., Thesis, Faculty of Science, Cairo University, Cairo (2004).

[30] Magdi Ibrahim Khalil, Thesis, Faculty of Engineering, Tanta University. (2004).

[31] Maayouf, R.M.A., *et al.,* Arab J. Nucl. Sci. Appl. 36 (2003) 127-131.

[32] Maayouf, R.M.A., *et al.,* Nucl. Inst. Meth. Phys. Res., Sect. A 484 (2002) 459-468.

[33] Magdi Ibrahim Khalil El-Sharqawy, Thesis, Faculty of Engineering, Benha University (2006).

[34] Maayouf, R.M.A., *et al.,* Arab J. Nucl. Sci. Appl. 37 (2004) 233-242.

[35] Maayouf, R.M.A., *et al.,* Kerntechnik 57 (1992) 270.

[36] Maayouf, R.M.A., *et al.,* Nucl. Inst. Meth. Phys. Res., Sect. A 349 (1994) 540.

[37] Maayouf, R.M.A., *et al.,* J. Nucl. Sci. 32 (1995) 79.

[38] Maayouf, R.M.A., J. Phys. Soc. Jpn., Suppl. A 65 (1996) 238-240.

[39] Maayouf, R.M.A., Physica, B 241, B 243 (1998) 89-91.

[40] Ebisawa, T., *et al.,* Physica, B 213, B 214 (1995) 901.

[41] Maayouf, R.M.A., *et al.,* Kerntechnik 63 (1998) 157.

[42] Maayouf, R.M.A., Physica, B 283 (2000) 340-342.

[43] Maayouf, R.M.A. Physica, B 291 (2000) 54-58.

[44] Anderson, H.L., 50th Anniversary Physics Vade Mecum (Conf., American Institute of Physics, New York) (1981) 316.

9. List of dissertations performed using the CFDF (supervised by Prof. Dr. R.M.A. Maayouf)

1) Neutron Spectrum Measurements Using Neutron Guide Facility.
M.Sc. Thesis by Ihab Abdel Latif Abdel Latif El-Sayed, Faculty of Science, Cairo Univ., 1997.

2) Study of the Optical Characteristics of the Neutron Guide at the ET-RR-1Reactor.
M.Sc. Thesis by Ashraf El-Kady, Faculty of Science, Ain Shams Univ., 1998.

3) Neutron Diffraction Measurements Using the Cairo Fourier Diffractometer Facility.
M.Sc. Thesis by Yasser El-Shaer, Faculty of Science, Zaqaziq Univ., 1999.

4) Measuring, Acquiring and Recording of the Neutron Flux Intensity at the Cairo Fourier Diffractometer.
M.Sc. Thesis by Magdi Ibrahim Khalil, Faculty of Engineering, Tanta Univ., 2003.

5) Fault Diagnosis Using Artificial Neural Network.
M.Sc. Thesis by Samah M. Abdelwahed, Faculty of Engineering, Ain Shams Univ., 2004.

6) Neutron Flux and Spectrum Measurements at the CFDF Using Different Detectors.
M.Sc. Thesis by Walaa M. El-Maamly, Faculty of Science, Zaqaziq Univ., 2004.

7) On the Use of the Cairo Fourier Diffractometer Facility for Neutron Diffraction Studies.
Ph.D. Thesis by Yasser El-Shaer, Faculty of Science, Cairo Univ., 2004.

8) A Data Acquisition System for the Cairo Fourier Diffractometer Facility Measurements.
Ph.D. Thesis by Magdi Ibrahim Khalil El-Sharqawy, Faculty of Engineering, Benha Univ., 2005.

Nuclear Data Section
International Atomic Energy Agency
Vienna International Centre, P.O. Box 100
A-1400 Vienna
Austria

e-mail: services@iaeand.iaea.org
fax: (43-1) 26007
telephone: (43-1) 2600-21710
Web: http://www-nds.iaea.org